BILINGUAL PUBLISHING CO.
Pioneer of Global Academics Since 1984

04

Journal of Geographical Research

Volume 2 | Issue 4 | October 2019 | ISSN 2630-5070 (Online)

BILINGUAL PUBLISHING CO.
Pioneer of Global Academics Since 1984

Volume 2 Issue 4 • October 2019 • ISSN 2630-5070 (Online)

Journal of Geographical Research

BILINGUAL PUBLISHING CO.

Pioneer of Global Academics Since 1984

BILINGUAL PUBLISHING CO.
Pioneer of Global Academics Since 1984

Volume 2 | Issue 4 | October 2019 | Page 1-29
Journal of Geographical Research

Contents

Article

BILINGUAL PUBLISHING CO.
Pioneer of Global Academics Since 1984

Journal of Geographical Research
https://ojs.bilpublishing.com/index.php/jgr

ARTICLE

Land Conversions and Forest Dynamics in a Riparian Forest Zone in South East Nigeria

Nwabueze I. Igu[1*] Joseph O. Duluora[2] Uzoamaka R. Onyeizugbe[2]

1. Department of Geography and Meteorology, Nnamdi Azikiwe University, Awka
2. Department of Environmental Management, Nnamdi Azikiwe University, Awka

ARTICLE INFO

Article history
Received: 26 November 2019
Accepted: 20 December 2019
Published Online: 30 April 2020

Keywords:
Climate change
Biodiversity conservation
Ecosystem services
Livelihoods
Sustainable forest use
Tropical ecosystems

ABSTRACT

The rate at which forest ecosystems are lost and modified across tropical landscapes are alarming, yet proper documentation and proactive measures to curtail this still remains a huge challenge in most areas. This research focused on elucidating the ongoing land use change patterns of a riparian forest landscape, its current impacts on the ecosystem and land surface temperature, as well as its likely future scenarios for the zone. LANDSAT images were downloaded for 1988, 2003 and 2018 and used to show the dynamics for the zone, its drivers and their varying temperatures. Maximum Likelihood Classification algorithm was used for the classification and the land-use classes were categorized as: Water body, Farms and Sparse Vegetation, Built-up Areas, Bare Surface, and Thick Vegetation. Furthermore, Markov Chain Analysis was employed for understanding the future patterns of land use change in the zone. Land use categories experienced changes over the three epochs, but among all, farmlands/ sparse vegetation and thick vegetation had the most significant changes from 7.70 to 58.67 percent and 73.56 to 20.58 percent, respectively; implying that much of the forestland use/cover (which constituted the bulk of the land initially; 73.56 percent) were converted to agricultural land use. This same trend at which agriculture grew in the zone was seen to affect the land surface temperature for zone (Pearson correlation coefficient of 0.99 with $p = 0.0058$ at 0.05 level of significance). Future projection for the zone equally showed that agricultural land use will likely dominate the entire landscape in the coming years and a consequent impact on the climate and ecosystem expected as well. On that note, intensive agricultural practices that seek to maximize allocated farm units were advocated. Such initiatives will help to ensure that agricultural growth is contained within delimited zones so that haphazard cultivations, reductions in ecological value of the forest landscape and consequent climatic impacts could be managed across the region.

1. Introduction

Much of the terrestrial ecosystem and their biodiversity have been altered across the globe. Land use change and intensification are to a large extent responsible for these changes globally [4] and for each spatial scale where they occur, consequent impacts abound. Such changes threaten forest biodiversity, responsible for the modification of spatial patterns

**Corresponding Author:*
Nwabueze, I. Igu,
Department of Geography and Meteorology, Nnamdi Azikiwe University, Awka;
Email: nwabuezeigu@gmail.com, nik.igu@unizik.edu.ng

 DOI: https://doi.org/10.30564/jgr.v2i4.1449

in forest landscapes and ultimately lead to biodiversity loss across spatial scales [11,12]. Though these changes affect ecosystems globally, they are quite significant across tropical landscapes. This is a major source of concern especially because tropical landscapes are incidentally where much of the terrestrial biodiversity are found [15] and so calls for concerted attention. Since such changes pose threats to the bulk of terrestrial biodiversity (which are found in tropical ecosystems) [7] and affect ecosystem services, functions and livelihoods that depend on them [8], it is imperative and needful that such concerns are addressed.

Disruptions going on in tropical ecosystem are thought to constitute a greater peril for global biodiversity than any other contemporary phenomenon [3,10,18] and have become a major concern because the bulk of ecosystem services especially carbon storage and climate regulation are dependent on it [9]. The pattern this is seen to occur vary across the tropics but on the whole, agriculture appears more prominent though with variations in what is being grown [1,14,19]. Such trends in modifications have grave concerns and consequences for tropical landscapes and endanger much of its biodiversity which are continually fragmented in a bid to pave way for a vast array of anthropogenic activities. Such patterns of change affect the African landscape in diverse ways and its attendant impacts are thought to vary according to the activities and the stochastic factors that define the varied ecosystems.

Land use change is growing in magnitude across Nigeria as in other tropical zones and as the population index continues to accelerate, so will the attendant environmental degradation associated with pressure on the ecosystems escalate as well. With agricultural land use occupying a major part of the global land surface area [2], Nigeria and south eastern part in particular are seen to follow similar trend, though at different proportions. Modifications and dynamics surrounding land use change in south eastern Nigeria are not known to receive attention in the interior or sub-urban zones and its riparian corridors possibly because the high population density and the attendant indices for which the zone are known of are not concentrated there. With this, the rate at which forests in the zone are converted to other land uses such as agriculture is not really accounted for and so no visible conservation strategy is carried out across the zone. In a bid to understand the magnitude of this ongoing process across the region, this study was focused on a local government area where agricultural activities have grown in recent time in relation to other land use change drivers. This study is aimed at assessing the drivers of land use change in the region; especially agricultural land use change in relation to other drivers within the region. It equally elucidates the land absorption and conversion rate, effects on land surface temperature and likely pattern of change expected in the future.

2. Materials and Methods

2.1 Study Area

The study region (Figure 1) is located within the humid tropics where mean annual rainfall varies between 1500mm to 22500mm. Temperature condition of the area is high with mean annual temperature range of 27^0 C to 28^0 C and a peak of about 35^0C between February and April [13]. It is characterized by a thick sequence of shale and sandstones formed in the Paleocene age. Soils that typify the zone are lithosol, juvenile soil, ferralitic soils and hydromorphic soils that formed under the dominant influence of the prevailing factors of geological formations of the study area [16]. It is known for its fertile soils which are seen as the underlying factor for much of the agricultural activities that dominate the zone. Crops such as yam, rice, maize and legumes are produced in large quantities in the region. Rice production have dominated the zone for a long time and with the establishment of the Anambra-Imo River basin authority, it has received much impetus and greater output.

Anyamelum is a land abundant zone and other activities aside agriculture such as trading and agro-allied industries have equally grown in magnitude across the zone.

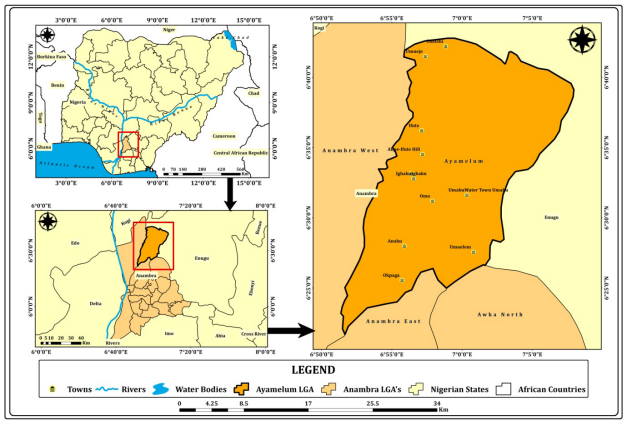

Figure 1. Map of the study area with the map of Anambra state and Nigeria inset

2.2 Data Collection

The medium resolution satellite data were downloaded from USGS Earth Explorer using the LANDSAT dataset module. The Thematic Mapper (TM) image was downloaded for 21st December, 1988. The Enhanced Thematic

DOI: https://doi.org/10.30564/jgr.v2i4.1449

Mapper plus (ETM+) image was downloaded for 24th October, 2003 and the Operational Land Imager (OLI) for 28th December, 2018. The Landsat satellite data have 30m spatial resolutions, and the TM and ETM+ images have spectral range of 0.45-2.35 micrometer (μm) with bands 1 to 7 and 8 respectively, while the Operational Land Imager (OLI) extends to band 11.

2.3 Image Classification

For the Landsat TM, ETM+ and OLI, a False Colour Composite (FCC) operation was performed using the ArcGIS 10.4 software and the images were combined in the order of band 5, 4 and 1 for Landsat TM and ETM+ while that of Landsat OLI was in the order of band 6, 5 and 3 due to change in sensor. The images were then clipped to the boundary of Ayamelum. A supervised classification scheme with the Maximum Likelihood Classification algorithm was used for the classification. The supervised classification was performed by creating a training sample, and based on spectral signature curve and visual interpretation. The following land-use classes were created: Water body, Farms and Sparse Vegetation, Built-up Areas, Bare Surface and Thick Vegetation.

2.4 Land Conversion Rate and Land Absorption Coefficient

Land Conversion Rate (L.C.R) is the measure of compactness which indicates a progressive spatial expansion of a city while Land Absorption Coefficient (L.A.C) is a measure of change in the consumption of new urban land by each unit increase in urban population [17].

The Land Conversion Rate (L.C.R) and Land Absorption Coefficient (L.A.C) was determined for the study area using the equations as shown below:

$$LCR = \frac{A}{P} \quad 1$$

where, A is the Areal extent of the study area in sq km
P is the Population

$$LAC = \frac{A_2 - A_1}{P_2 - P_1} \quad 2$$

where, A1 and A2 are the areal extents for the early and later years, while P1 and P2 are their population, respectively.

The growth rate used for estimating the population of Ayamelum LGA was determined to be 2.67%. The equation used is given as:

$$P_t = P_o \times (1 + \frac{r}{100})^t \quad 3$$

Here, t = number of years; Pt= Population after 't' years; Po= Population at the start; r = the annual growth rate.

2.5 Land Surface Temperature

Land surface temperature of the zone for the three years: 1988, 2003 and 2018 were extracted from the Landsat remote sensing lab.gr site for the month of February/March for the years under review. Mean temperature for 1988 was downloaded for 7th February, that of 2003 was downloaded for 4th March and that of 2018 was downloaded for 1st February.

2.6 Future Projection

Markov Chain Analysis being a convenient tool for modelling land use change was employed for understanding the future patterns of land use change in the zone since its process allows the future state of a system to be modelled purely on the basis of the immediately preceding state. It describes land use change from one period to another and uses this as the basis to project future changes [20]. This was used to predict the land use land cover (LULC) situation in each LULC type for the year 2028 based on the 2003-2018 scenarios in Ayamelum. The 10 (ten) year LULC projection for the future was done using Markov chain model incorporated in the IDRISI-SELVA software. The change between 2003 and 2018 was used as the basis for the prediction. The results were displayed in a table, and were converted to square kilometres from pixel count. This was done to enable easy discussion.

Pearson correlation was used to show the relationship between agriculture (farmlands) and land surface temperature (LST) of the zone.

3. Results and Discussion

Land use and land cover changed significantly over the years under review. These are presented in the following imageries:

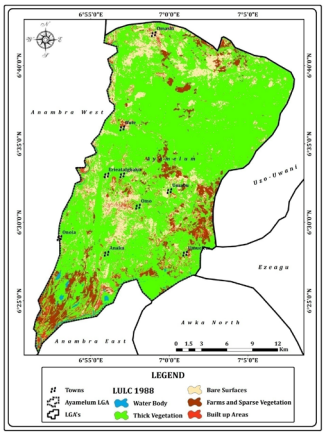

Figure 2. Land use and land cover change for 1988

 DOI: https://doi.org/10.30564/jgr.v2i4.1449

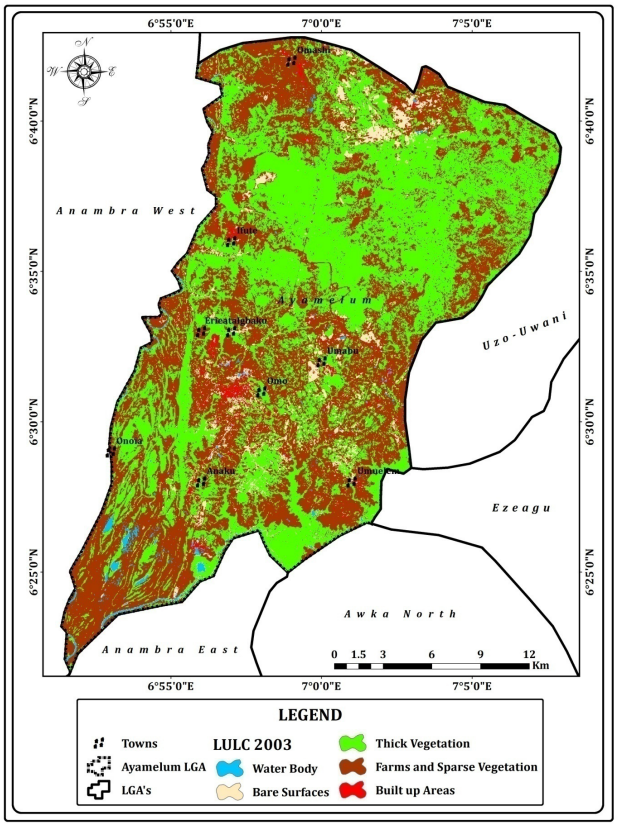

Figure 3. Land use and land cover change for 2003

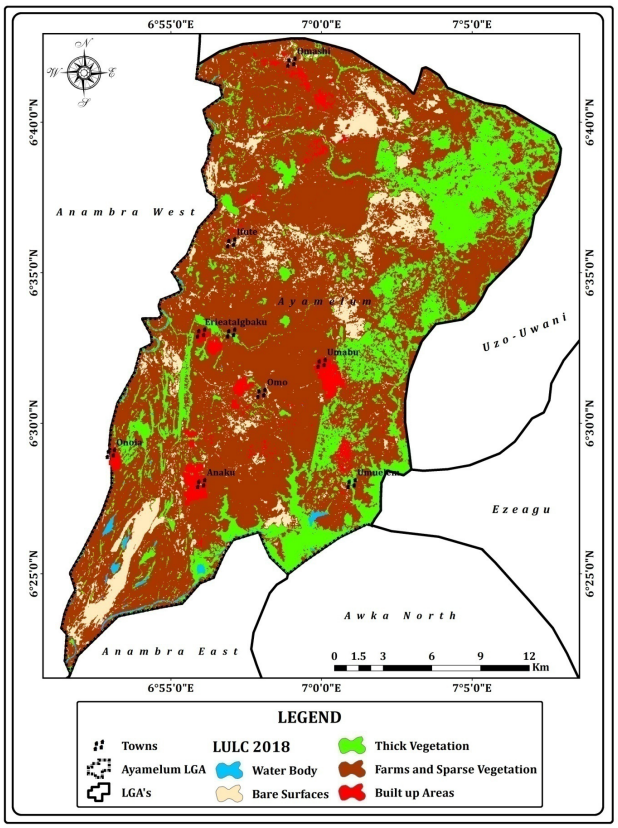

Figure 4. Land use and land cover change for 2018

A summary of all the changes encountered throughout the period is given in the table below:

Table 1. Total detection for land use and cover changes from 1988 - 2018

Class Name	Initial year 1988	**1988 to 2003**	**2003 to 2018**	**1988 to 2018**
Water Body	3.44	-0.25	0.56	0.31
Bare Surfaces	94.03	-37.46	21.09	-16.37
Thick Vegetation	434.74	-148.13	-164.99	-313.12
Farms and Sparse Vegetation	45.51	169.74	131.49	301.23
Built up Areas	13.24	16.17	11.57	27.74

The area under study changed visibly over the years (1988 – 2018) with some land uses recording more changes than others. Water body, bare surfaces and built up areas both increased and decreased slightly over the study period. They did not have significant variations in total land areas and were not the major causes of land use change in the region (Figure 2- 4). The fluctuations in the area of land covered with water were mainly from the variations experienced in flooding in the zone per year. Being a swampy and flood prone zone that experiences a yearly flooding regime, it was characterized by variations in the area of land that were inundated with water yearly; with some years experiencing more or less volume of flood water than another. On the other hand, bare surfaces reduced in the area of coverage between 1988 – 2003, but increased between 2003 – 2018. Such areas with little or no vegetation cover are rarely used for agricultural purposes in the zone and are at the risk of becoming more parched as the micro climate of the zone changes over time. Since the area has ample parcels of land which are increasingly turned into agricultural lands, much thought is not given to the reclamation of the land for such purposes and so are allowed to lie fallow.

Built up areas equally increased over the study period but did not have much impact in terms of land use alterations in the zone. As at the initial year of 1988, it occupied 13.24 sq km of the land area and increased up to 27.74sq km by 2018. It meant that the population of the area only grew gradually and there were not much need for housing units as would be seen in urban areas. This further explains why the land conversion rate and land absorption coefficient as at 2018 were only 0.000196 and 0.000226, respectively. On the other hand, it equally meant that the increasing scale of agricultural activities could not have been promoted only by people living within the area, but also from interested stakeholders who operate from outside the zone and have no need of rooming

DOI: https://doi.org/10.30564/jgr.v2i4.1449

space in the locality.

Agricultural activities had much impact in the area and were to a great extent responsible for the reduction of thick vegetation in the zone to sparse vegetation. Alongside sparse vegetation, farmlands were seen to increase from the initial year size of 45.51sq km to 301.23sq km by 2018 (Figure 2- 4). Conversely, thick vegetation lost much of its extent and cover (mainly to agricultural land use) as it was seen to lose as much as 313.12sq km between 1988 to 2018. (Figure 2 -4).

Projected change in land use and cover (table 2) showed that while modifications in land use are expected for the different categories, farms and sparse vegetation will still constitute the most extensive land use in terms of land coverage.

Table 2. Projected land use and cover change for 2028 being the next 10 years from 2018

	Probability of changing to in sq. km.				
Given Class	**Water Body**	**Built up Areas**	**Bare Surface**	**Farms and Sparse Vegetation**	**Thick Vegetation**
Water Body	0.11	0.04	0.28	1.12	4.73
Builtup Areas	0.001	23.42	4.5	3.84	1.3
Bare Surface	0.26	19.61	20.72	18.14	5.69
Farms and Sparse Vegetation	0.94	37.4	8.41	43.06	31.13
Thick Vegetation	1	7.27	13.83	33.26	27.03

Land surface temperature for the period under review showed increased mean temperatures of 29, 33 and 36^0C for 1988, 2003 and 2018, respectively.

Implications for Land Conservation and Regional Climatic Patterns

Land use across the zone changed mainly due to agricultural activities and affected the capacity and extent of other land use categories. Though agricultural expansion is a global phenomenon, it continues with less restraint or modification in land consumption/absorption pattern in the zone as in many parts of Africa because of the notion that land is abundant [6]. This location has much unoccupied land than is normally the case in many parts of Anambra state where it is located; hence, acquiring more land seemed easier over the years. Such land acquisitions and extensions were done at the expense of the forests (thick vegetation) which shrunk in size as the farmlands increased; with consequent losses and impacts on the biodiversity of the zone.

There is need to utilize the already existing farmlands maximally rather than a haphazard and quick conversion of the vegetation thick zones to farmlands. Since the conversions have been unregulated and uncoordinated to a large extent, the remaining sparse vegetation found within the converted zones occurs as tiny mosaics with almost no ecological value and conservation prospects. This could have been much avoided if agricultural intensification is much promoted in the zone. Such initiatives ensures that farmers utilizes the available farmlands maximally by improving soil fertility and engaging improved farming techniques within the parcels of land where they already farm [5]. On the other hand, farming plots should be planned, properly apportioned and monitored, even if they have ample agrarian farm lands in the zone. This will help to reduce forest fragmentation and equally ensure that the remaining forest patches (though small) are together and become more ecologically useful.

Results of the correlation between agricultural land use and land surface temperature showed a strong relationship of 0.99 ($p = 0.0058 < 0.05$ level of significance). This meant that as the vegetation cover of the zone declined over the years; it affected (increased) the land surface temperature of the area. Vegetation cover reduces the direct impact of sun in a zone and in turn reduces or normalizes the temperature of an area. The reverse becomes the case when the vegetation of such a zone become so sparsely distributed or in extreme cases, are turned into zones that is bare of vegetation. Future land use projections for the area showed that more vegetation dense zones will be converted to other land uses such as agriculture and built up areas (table 2) and by implication suggests that the micro climate will become altered. Since these are grave concerns facing the zone, there is then every need to engage in climate friendly agricultural innovations that will accommodate both agricultural and climate regulation initiatives.

4. Conclusion

Land use and cover across many tropical landscapes are undergoing changes and modifications as a result of varied forcings. As it concerned the region under review, such changes were mainly as a result of the increase in the area of land under cultivation. This was to a great extent responsible for the loss of thick vegetation, subsequent modification to sparse vegetation and increase in land surface temperature for the zone. Reducing encroachment to forest areas and engaging in climate friendly and resilient strategies for agriculture and building purposes will help reduce loss of more forest areas and adverse climatic impacts for the region.

References

[1] Abood S. A., Lee J. S. H., Burivalova Z., Gar-

 DOI: https://doi.org/10.30564/jgr.v2i4.1449

cia-Ulloa J., Koh L. P.. Relative contributions of the logging, fiber, oil palm, and mining industries to forest loss in Indonesia. Conserv. Lett., 2015, 8: 58–67.

[2] Asai, M., Reidsma, P., Feng, S.. Impacts of agricultural land-use changes on biodiversity in Taihu Lake Basin, China: a multi-scale cause-effect approach considering multiple land-use functions. International Journal of Biodiversity Science, Ecosystem Services and Management, 2010, 6(3-4): 119-130.

[3] Bradshaw, C.J.A., Sodhi, N.S, Brook, B.W.. Tropical turmoil- A biodiversity tragedy in progress. Front. Ecol. Environ, 2009, 7: 79-87.

[4] Butchart, S. H. M., Walpole, M., Collen, B., van Strien, A., Scharlemann, J. P. W., Almond, R. A. E., Baillie, J. E. M., Bomhard, B., Brown, C., Bruno, J., Carpenter, K. E., Carr, G. M., Chanson, J., Anna, M.. Global biodiversity: indicators of recent declines. Science, 2010, 328(5982); 1164-1168.

[5] Byerlee, D., Stevenson, J., Villoria, N.. Does intensification slow crop land expansion or encourage deforestation? Global Food Security, 2014, 3: 92-98.

[6] Chamberlin, J., Jayne, T. S., Headey, D.. Scarcity amidst abundance? Reassessing the potential for cropland expansion in Africa. Food Policy, 2014, 48: 51-65.

[7] Gardner, T.A., Barlow, J., Chazdon, R., Ewers, R.M., Harvey, C.A., Peres, C.A., Sodhi, N.S.. Prospects for tropical forest biodiversity in a human-modified world. Ecology Letters, 2009, 12: 561-582.

[8] Igu, N. I.. Swamp forest use and loss in the Niger Delta: Contextual and underlying issues. Open Journal of Forestry, 2017, 7: 34-47.

[9] Igu, N. I., Nzoiwu, C. P., Anyaeze, E. U.. Biodiversity and carbon potentials of a Nigerian forest reserve: Insights from the Niger Basin. Journal of Environmental Protection, 2017, 8: 914-922.

[10] Laurance, W.F., Useche, D.C., Rendeiro, J., Kalka, M., Bradshaw, C.J.A., Sloan, S.P., Laurance, S.G., Campbell, M., et al.. Averting biodiversity collapse in tropical forest protected areas. Nature , 2012, 489: 290-294.

[11] Lindenmayer, D.. Land use intensification in natural forest settings. In: Lindenmayer, D., Cunningham, S., Young. A. (Eds) Land use intensification: effects on agriculture, biodiversity and ecological processes. CSIRO Publishing, Australia, 2012: 113-121.

[12] Lindenmayer, D. Interactions between forest resource management and landscape structure. Current lands Ecol Rep. 2016, 1 (1): 10-18.

[13] Monuanu, P.C.. Temperature and sunshine, in: Ofomata, G.E.K(ed). Nigeria in Maps: Eastern states. Ethiope, Publishing House, Benin City,1975.

[14] Nepstad D., McGrath D., Stickler C., Alencar A., Azevedo A., Swette B., Bezerra T., DiGiano M., Shimada J., Seroa da Motta R., Armijo E., Castello L., Brando P., Hansen M. C., McGrath-Horn M., Carvalho O., Hess L.. Slowing Amazon deforestation through public policy and interventions in beef and soy supply chains. Science, 2014, 344: 1118–1123.

[15] Norris, K.. Agriculture and biodiversity conservation: opportunity knocks. Conservation Letters, 2008, 1: 2-11.

[16] Ofomata, G.E.K.. Nigeria in Maps: Eastern States .Ethiope, Publishing House, Benin City, 1975.

[17] Paria, P. and Bhatt, B.. A spatio-temporal land use change analysis of Waghodia taluka using RS and GIS. Geosci. Res, 2012, 3 (2): 96-99.

[18] Pimm, S.L. and Raven, P.R.. Biodiversity: Extinction by Numbers. Nature, 2000, 403: 843-845.

[19] Tyukavina, A., Hansen M. C., Potapov, P., Parker, D., Okpa, C., Stehman, S. V., Kommareddy, I., Turubanova, S.. Congo Basin forest loss dominated by increasing smallholder clearing. Science Advances, 4, 2018, 2993: 1-12.

[20] Zubair, A. O.. Change detection in land use and land cover using remote sensing data and GIS: A case study of Ilorin and its environs in Kwara state. M.Sc thesis, University of Ibadan, Nigeria, 2006.

DOI: https://doi.org/10.30564/jgr.v2i4.1449

BILINGUAL PUBLISHING CO.
Pioneer of Global Academics Since 1984

Journal of Geographical Research
https://ojs.bilpublishing.com/index.php/jgr

ARTICLE

Effect of Precipitation Characteristics on Spatial and Temporal Variations of Landslide in Kermanshah Province in Iran

Safieh Javadinejad[1*] Rebwar Dara[2] Forough Jafary[2]

1. Department of Geography, Earth and Environmental Sciences, University of Birmingham and University of Tehran, Edgbaston St., B152TT, United Kingdom
2. Department of Geography, Earth and Environmental Sciences, University of Birmingham, Edgbaston St., B152TT, United Kingdom

ARTICLE INFO

Article history
Received: 20 April 2020
Accepted: 28 April 2020
Published Online: 30 April 2020

Keywords:
Characteristics of precipitation
Effects
Landslide
Movement
GPS

ABSTRACT

Landslide can be defined as the mass movement of sloping slopes under the influence of mass gravity and its stimuli such as earthquakes, floods and flood plains. This phenomenon is one of the natural hazards that every year causes a lot of financial and financial losses in mountainous, rain-fed and seismic areas. Detection of time and the magnitude of landslides are necessary to understand the causes of landslide and to warn potential hazards. In this research, the amount of landslide displacement in Kermanshah province was evaluated by the characteristics of rainfall. To this end, a network of fixed points in and out of the slipping mass of 20 points was created to monitor the amount of displacement on different slip load users and the amount of displacement of each point in 5 time intervals using the Global Positioning System for two-dimensional GPS measurement. The results of the 511-day follow-up showed that the total horizontal displacement of the moving points in the 5 intervals measured at 1658 mm has a monthly displacement rate of 112 mm. Also, the total vertical displacement of moving points at the same time is 899 mm, with a monthly movement rate of 71 mm. Then, precipitation variances such as rainfall, rainfall, precipitation duration, maximum rainfall intensity in the intervals of 10, 20, 30 and 60 minutes and the average rainfall intensity were calculated and extracted for each of the 5 time periods. The drawing of the vectors of points on the topographic map of the area indicated that the direction of mass movement is in the direction of elevation gradient of the region. The results showed that only the precipitation severity with the landslide had a good correlation. The landslide movement had the highest correlation with average rainfall intensity (R = 0.85) and with maximum 30 minutes rainfall (R = 0.67), respectively, and other rainfall characteristics like amount, duration, and type of rainfall had not significantly correlated with movement of landslides.

**Corresponding Author:*
Safieh Javadinejad,
University of Birmingham, Edgbaston St., B152TT, UK;
Email: nsofiya65@gmail.com; javadinejad.saf@ut.ac.ir

 DOI: https://doi.org/10.30564/jgr.v2i4.1818

1. Introduction

Dominant and landslide instabilities occur for several reasons. In this regard, the role of the intensity and duration of the landing is important for the beginning of the slip, so that today rain is known as the most common cause of landslides [2]. Hong et al. [5] also considered the role of hydrologic factors such as rainfall, soil moisture, subsurface flow and underground water depth in the stability or un-stability of various natural and artificial slopes, and stated that climate change such as increase Extreme and short-term rainfall, due to mild and long-term precipitation, is a factor in increasing landslides and damage caused by them. Rossi et al. [11] by analyzing rainfall data for long and short daily and hourly periods, it was concluded that heavy rainfall in the landslide has a role as a stimulant. Pham et al. [10] also found that at any time during the rainy season, the threshold of precipitation will exceed 682 mm, slip movements will occur. Also, Lin et al. [8] analyzed the landslide mechanism in the Taiwan, saying that extreme intensity and cumulative events of precipitation may be a large-scale and complex event causing disaster. Nevertheless, few studies have been conducted on the role of rainfall agent in landslide due to the lack of landslide data and the continued record of rainfall data globally [9]. Given that earth-landslide moving data is important for researchers in this science to evaluate the deformation stages and the rules of landslide motion, the Global Positioning System and computer science can be used as a tool to observe the amount of landslide displacement [7]. In their studies, observations of the global positioning system have replaced the size of the system in order to ensure the safety of the village, reduce the risk of investment and prevent earthquakes. The commonly used surveys are mapped and now play an important role in monitoring the variation of the surface of the earth. Huang et al. [6] used the observation of the GPS control station to investigate the subsidence of the mine and concluded that the observations of the GPS control network were accurate and highly efficient and could provide reliable data for analyzing the displacement and changes due to mining. Setiawan et al. [12] studied the status and controled of the landslide of a dam in Japan, designed and constructed the network point of this landslide in November 2016 and with six stages studied the planetary networks and the altitude of the landslide. The results showed that landslide movements with acceptable accuracy indicate the movement of the area towards the dam lake is relatively high, which is not the same for different parts of the mass; therefore, the relationship between intensity, duration and type of rainfall on the amount of landslide is monitored and Determining the direction of landslide with the help of the Global Positioning System GPS can be a turning point in the sustainable management of this natural disaster.

2. Study Area

The location of the study area is shown in figure 1. Because of the mountainousness and the relatively high slope of the area, there is a potential for ground thrust [4]. This landslide occurred in 1163, with an area of about 12 hectares between the coordinates of 45.5° and 48° E longitude and 33.7° and 35.3° N latitude (the parallels that cut across the Mediterranean Sea and southern United States) and the landslide in this area passes through a distance of 62 meters from the power village and damaged the road, electricity rails, part of the gardens and agricultural lands of the village. The height of the landslide from the free sea level varies from 1312 to 0122 meters. The main part of precipitation is snowy in the winter season and its melting in spring and summer provides the main source of water in the rivers of the region. Due to the favorable weather conditions and abundance of surface waters in the upstream slopes of the fruit gardens and they have been constructed on a large scale which is irrigated traditionally. On the forehead of this landslide, an abyssal slope with an altitude of more than 82 meters was created and up to a radius of about 122 meters, it formed seams and severe cracks in the asphalt road and agricultural lands located on the upstream landslide.

3. Materials and Methods

After identifying the slipper mass, the spatial displacement of the slipper mass was measured through the creation and measurement of a precise position of the network of points inside and outside the slippery mass in 7 time intervals. The data on the amount of precipitation and its characteristics such as average rainfall, snow depth, average rainfall, and maximum rainfall were calculated at 10, 20, 30 and 60 minutes, and the total precipitation time was calculated for each 7 time periods. Finally, the relationship between the amount of displacement and rainfall characteristics was determined by determining the vertical and horizontal displacement of 15 points in the range of observation in 7 time intervals and precipitation periods for each time interval.

3.1 Identify and Plot the Slider Area on Google Earth and Prepare a Topographic Map

First, the area slip on the Google Earth and the overall information from the area and the slippery range was achieved. After field inspection and removal of the slippery range with a manual GPS device, the target area was

DOI: https://doi.org/10.30564/jgr.v2i4.1818

transferred to the map of the inheritance and traced. It was also observed in desert visits that severe seams and cracks were created in a wide range of neighboring landslide landscapes that are likely to move in the future, which is why the range was also identified on Google Earth. Also, in order to provide a general view of the area and design of the monitoring points network and to identify the slope of each slope, which is one of the main causes of landslides, the topographic map of the slipping range with 1 meter elevation lines was prepared by land survey in 2015.

3.2 Studies of Land Slide Lithology

The sloping mass of the Madstone and Siltstone (related to the Miocene period is the Cenozoic era), and consists of rocks of rustic clay that are reddish and very fine grained. In terms of lithology, the sedimentary sequence is such that the layers of sandstone layers and The reddish conglomerate includes the Paleocene age of the Cenozoic stratigraphy, which is resistant to erosion, and in some parts has a thick layer. The complex of this structure, due to its high formability, tolerates intense corrosion and In general, the area is less visible horizontally. In fact, the mastonne and silt Columns that have high water absorption capacity have a background for landslide in the slab in the form of contiguous layers on a resistant layer and with low permeability of sandstone and conglomerate, along with a high slope and irrigation of the upland gardens. Covering these rocky units and providing these conditions that increase the forces of the actuator and reduce the forces of resistance, the possibility of the slab of the reddish stone unit on the sandstone will be very high.

3.3 Determine the Amount of Slippage Displacement by Creating a Behavioral Measurement Network

In the method of using two-dimensional global positioning systems, the position of the platforms installed on the slip surface on three axes X, Y and Z is calculated at specified intervals and, by analyzing the information, the mechanism of the landslide motion is evaluated. In this study, to monitor the spatial displacement of the slippery mass, a network of fixed points inside and outside the slipped mass was first created, and the precise position of each point in 7 time periods was measured using GPS.

Outside of the landslide area, 3 stations were established as a reference framework and a point network, whose strength was controlled by daily observation of the geodynamic station of the region, whose exact coordinates are determined and controlled daily by the Surveying Organization of the country. A total of 17 control stations were established in order to measure the slipping mass in critical points of the landslide surface with regard to the location of gaps, gaps and suspicious masses and to measure landslide motion. The grid points were selected in such a way that they provide a complete coverage of the driven area along with relative strength.

To determine the displacement of network points, consecutive observations of the monitored points were compared. The spatial variations of the control points in the slippery area were compared to 3 solid points outside the mass during 3 stages in 2015 and 2016, and 4 stages in 2017 and 2018 (3 time intervals by GPS).

Also, by calculating the relative elliptical error ellipse occurred at each point, the meaning of displacements in the dimension of the levels was determined so that if the movement vector was placed inside this ellipse, the analysis would be non-displacement, otherwise the analysis would lead to displacement.

3.4 Weather Data Analysis of Rain-gauge Station

To determine the relationship between rainfall characteristics and the amount of landslide movement, the data were takenat the base of the time of 10 minutes from the rain gardener located at 8 km of the study area was obtained. Also, the monthly statistics of the meteorological station, where snow depth is available in cm, was obtained from the meteorological station in order to determine the relationship between the type of precipitation and the landslide. In order to investigate the relationship between rainfall characteristics and the amount of landslide movement, firstly, the characteristics of each time interval such as average rainfall, as well as maximum precipitation time of 10, 20, 30 and 60 minutes, as well as snow height, average rainfall, and also the total precipitation time was calculated for each time interval. Also, to determine the relationship between precipitation patterns and the amount of displacement, first, the rainfall events less than 2 mm were calculated due to the lack of runoff from the data, and then the remaining features of rainfed events were calculated.

4. Results

4.1 Determination of the Plane and Elevation of Observational Data

At this stage, the difference in the coordinates of two consecutive observation periods was compared and the displacement of the planes and the height of 17 control points in the slip area in the AutoCAD environment were calculated as shown in table 1 to 5.

 DOI: https://doi.org/10.30564/jgr.v2i4.1818

4.2 Draw Vectors of Displacing Points on a Topographic Map

After determining the displacement values and directions for moving points, the position of the points of measurement on the topographic map of the foot area and the amount of displacement of points with exaggeration and on another scale in the calculated directions were drawn as directional vectors with their error oval. The minimum and maximum displacement vector of the points of observation with its opaque error on a part of the area are shown in figure 2 and 3.

4.3 Relationship of Rainfall Characteristics and Displacement Rate of Slipping Mass

Over the entire study period, a total of 65 incident occurrences, with a rainfall of more than 2 mm, or 52 cases. The characteristics of the maximum precipitation intensity of 10,20,30 and 60 minutes and the average rainfall, as well as the amount of precipitation, snow depth, the total duration of precipitation for each time interval were calculated and, finally, the correlation coefficient of the maximum rainfall intensity with its other characteristics with the average The horizontal and vertical displacement of points related to the same interval was determined. The results showed that among all the characteristics of rainfall, only the characteristics related to rainfall intensity, are more correlated with the mean horizontal and vertical displacement of 7 time intervals. But the rest of the precipitation properties did not show a good relationship with the displacements of the points.

5. Discussion

In this study the effects of rainfall characteristics on landslide is analyzed. It's very important to apply GPS and effects of rainfall characteristics in the landslide hazard research field and it could become a major tool for analyzing landslides that occur in the region.

However, previous studies did not consider this effect in Iran. Alcántara et al. [1], studied landslides around the world, visiting sites and analyzing post-landslide data. However, their study did not include Iran areas. Their study showed that the landslide happened on an active fault line that is creeping at a rate of 2.5 centimeters (1 inch) per year in specific areas. That might seem gentle, however over time the movement grinds and breaks up the rock, affecting the stability of surrounding slopes and making them more prone to landslides. Their results showed that tectonic weakening was a preconditioning element making that slope vulnerable to catastrophic failure.

They applied their ground observations to validate what they had observed in remotely sensed data. However, they only analyzed vertical movement of landslide. Nevertheless, this current study analyzed both vertical and horizontal movement of landslide.

In order to investigate rainfall as a potential factor that effect on landslide, Yang et al. [14] considered satellite imagery from TRMM. The TRMM image revealed that, in tropical area, more than sixty-eight centimeters (twenty-seven inches) of rain had fallen between February 4, 2006, and February 17, 2006. This was excessive rainfall beyond the monthly averages—more than twice as much that probably cause landslide. However, other rainfall characteristics did not consider in their study.

In addition, Ciabatta et al. [3] participated to the development of the TRMM Real-Time Multi-Satellite Precipitation Analysis (TMPA-RT) product. The TMPA-RT data, presently available online from 2002 through the present, are updated in real time, permitting users to measure if a region is currently receiving particularly intense rainfall or has reached a critical level of accumulation. However, the data is limited and not available for all countries and all regions.

Furthermore, a research on world assessed TMPA-RT data to help gauge precipitation and flooding in more than 250 river basins worldwide. It may also help to analyze landslide events [13].

Developing the TMPA-RT system can be more useful to local governments and organizations on the ground to analyze landslide movement for all regions in the world. As with many mountainous areas in the world, timely landslide hazard assessment may be difficult to accomplish without satellite data. This system will be valuable when national and international organizations must plan disaster mitigation or relief work. It can give them quantitative information about where exactly the hazard is and which areas are affected. So, for future research, analyzing the characteristics of precipitation with TMPA-RT system can recommend.

6. Conclusion

In this paper, the relationship between rainfall characteristics such as severity, amount, duration and type of precipitation on the landslide displacement in Kermanshah province was investigated. The results of the analysis of observations and the analysis of the displacement of points in 7 time intervals showed that relative displacement occurred between some points in the network. By drawing the vectors of moving points on the topographic map of the region, the direction of mass movement is in the direction of the general slope of the region. Meanwhile,

DOI: https://doi.org/10.30564/jgr.v2i4.1818

although there are vertical and horizontal displacements between all the points of the network within the landslide range, there is a significant decrease in the displacement at the margins of points 1, 2, 4 and 8. The total amount of horizontal displacement of the moving points in 5 periods of time of observation is 1900 mm, with a monthly movement rate of 112 mm. Also, the total amount of vertical displacement of moving points at the same time is 736 mm with a monthly displacement rate of 51 mm. The results showed that among the different precipitation characteristics, only the rainfall intensity and slip density mass ratios are in good agreement. The previous studies also Similar results were obtained regarding the effective role of precipitation and the relationship between precipitation intensity and landslide occurrence. The highest correlation coefficient is between the average rainfall and the maximum rainfall of 30 minutes with the horizontal displacement of the slipper mass. There was no significant relationship between other characteristics of rainfall, such as amount, duration and type of precipitation, including snow or rain, and the amount of slippage mass. In general, it can be concluded that the effect of different factors such as topography, soil formation, geology, use and precipitation severity Has created favorable conditions for the slippage of the slipping mass in the area, but in this landslide, the effective role has been played by the intensity of precipitation.

Declaration

Competing Interests

"The authors declare that they have no competing interests."

Funding

We thank Regional Water Authority for funding this study to collect necessary data easily and helped the authors to collect the necessary data without payment, Mohammad Abdollahi and Hamid Zakeri for their helpful contributions to collect the data. All other sources of funding for the research collected from authors.

Authors' Contributions

Safieh Javadinejad designed this research and she wrote this paper and she collected the necessary data and she did analysis of the data.

Rebwar Dara participated in drafted the manuscript and he contributed in the collection of data and interpretation of data and edited the format of the paper under the manuscript style.

Forough Jafary participated in the data collected and data analysis.

Acknowledgements

Funding

We thank Esfahan Regional Water Authority for funding this study to collect necessary data easily and helped the authors to collect the necessary data without payment, Mohammad Abdollahi and Hamid Zakeri for their helpful contributions to collect the data. All other sources of funding for the research collected from authors. We thank Forough Jafary who provided professional services for check the grammar of this paper.

Supplements

List of Tables

Table 1. Network displacement values of points in the 175-day intervals of the first and second stages of observations (2015-2016)

Situation of vertical movement	Situation of horizontal movement	**Vertical movement (mm)**	**Horizontal movement (mm)**	**Movement on y axis (mm)**	**Movement on x axis (mm)**	**Number of point**
Movement happened	Movement happened	-26	34	-30	-17	1
Movement happened	Movement happened	-48	131	6	-130	2
Movement happened	Without movement	-15	2	2	2	3
Movement happened	Without movement	-13	6	-4	5	4
Movement happened	Without movement	-17	6	2	-7	5
Movement happened	Movement happened	-19	37	-35	-13	6
Without movement	Movement happened	7	10	-10	-4	7
Movement happened	Movement happened	-26	40	-32	-24	8
Movement happened	Without movement	-16	6	3	6	9
Without movement	Movement happened	-11	11	3	-11	10
Movement happened	Without movement	-15	5	-5	0	11
Movement happened	Movement happened	-21	6	-5	-4	12
Without movement	Movement happened	6	11	-8	-8	13
Movement happened	Without movement	-15	5	-2	4	14
Without movement	Movement happened	-9	12	-11	-3	15
Without movement	Movement happened	-14	11	-8	9	16
Without movement	Movement happened	10	22	-5	-22	17

 DOI: https://doi.org/10.30564/jgr.v2i4.1818

Table 2. The values of the network of control points in the 102-day intervals of the second and third stages of the year(2015-2016)

Situation of vertical movement	Situation of horizontal movement	Vertical movement (mm)	Horizontal movement (mm)	Movement on y axis (mm)	Movement on x axis (mm)	Number of point
Movement happened	Movement happened	-24	161	-143	-74	1
Movement happened	Movement happened	-113	168	4	-168	2
Without movement	Without movement	19	7	-5	-6	3
Without movement	Movement happened	6	16	-2	-15	4
Without movement	Without movement	2	6	-5	5	5
Without movement	Movement happened	-4	164	-160	-37	6
Movement happened	Without movement	-22	3	-2	-2	7
Movement happened	Movement happened	-83	244	-217	-112	8
Without movement	Without movement	7	6	-3	-6	9
Without movement	Without movement	-2	6	-5	6	10
Without movement	Movement happened	15	13	4	-12	11
Without movement	Without movement	7	4	-3	-4	12
Movement happened	Without movement	-25	12	12	5	13
Without movement	Without movement	-2	7	-2	-7	14
Without movement	Without movement	2	8	6	-7	15
Without movement	Without movement	-7	8	5	-7	16
Movement happened	Without movement	-25	10	7	8	17

Table 3. Networking values of points in the 70-day time interval of the first and second stages of the year 2017 and 2018

Situation of vertical movement	Situation of horizontal movement	Vertical movement (mm)	Horizontal movement (mm)	Movement on y axis (mm)	Movement on x axis (mm)	Number of point
Without movement	Without movement	-12	20	-18	-8	1
Without movement	Without movement	-19	19	-6	-18	2
Without movement	Without movement	-17	9	-9	2	3
Without movement	Without movement	11	17	-17	-6	4
Without movement	Without movement	-14	9	-5	8	5
Without movement	Without movement	-16	24	-21	-11	6
Without movement	Without movement	-10	12	2	12	7
Without movement	Movement happened	-25	47	-46	6	8
Without movement	Without movement	-13	9	6	7	9
Without movement	Without movement	-15	9	6	7	10
Without movement	Without movement	13	20	5	-19	11
Without movement	Without movement	-16	7	-6	-4	12
Without movement	Without movement	-19	17	-15	-8	13
Without movement	Without movement	-7	6	2	6	14
Without movement	Without movement	-8	10	-8	-6	15
Without movement	Without movement	-13	15	-15	-4	16
Without movement	Without movement	10	10	-9	-5	17

Table 4. Network displacement values of points in the 106-day period of the second and third stages of observations of 2017 and 2018

Situation of vertical movement	Situation of horizontal movement	Vertical movement (mm)	Horizontal movement (mm)	**Movement on y axis (mm)**	**Movement on x axis (mm)**	**Number of point**
Without movement	Movement happened	-27	73	-73	-5	1
Movement happened	Movement happened	-52	116	-28	-113	2
Without movement	Without movement	15	11	-4	11	3
Without movement	Without movement	-12	15	-7	-14	4
Without movement	Without movement	-6	9	8	6	5
Without movement	Movement happened	12	68	-68	-7	6
Without movement	Without movement	11	9	-9	0	7
Movement happened	Movement happened	-44	55	-55	5	8
Without movement	Without movement	13	15	-9	-13	9
Without movement	Without movement	-6	8	-7	-5	10
Without movement	Without movement	-23	10	-10	5	11
Without movement	Without movement	-14	11	-11	0	12
Without movement	Without movement	-16	16	9	14	13
Without movement	Without movement	8	5	2	5	14
Without movement	Without movement	-17	12	2	12	15
Without movement	Without movement	-14	14	-8	12	16
Without movement	Without movement	-28	14	-5	-13	17

DOI: https://doi.org/10.30564/jgr.v2i4.1818

Table 5. Network displacement values of points in the 78-day period of the third and fourth stage of observations of year 2017 and 2018

Situation of vertical movement	Situation of horizontal movement	Vertical movement (mm)	Horizontal movement (mm)	Movement on y axis (mm)	Movement on x axis (mm)	Number of point
Without movement	Movement happened	-25	77	-57	-53	1
Movement happened	Movement happened	-88	138	11	-137	2
Without movement	Without movement	-20	8	-6	-6	3
Without movement	Without movement	17	13	-13	-4	4
Without movement	Without movement	-11	10	-6	8	5
Without movement	Movement happened	-18	100	-88	-22	6
Without movement	Without movement	-18	10	4	9	7
Movement happened	Movement happened	-47	100	-98	-21	8
Without movement	Without movement	-20	18	-15	11	9
Without movement	Without movement	-12	10	-9	4	10
Without movement	Without movement	13	11	10	6	11
Without movement	Without movement	10	4	3	-2	12
Without movement	Without movement	-4	22	-21	-9	13
Without movement	Without movement	-30	11	-8	-8	14
Without movement	Without movement	-14	11	-10	-4	15
Without movement	Without movement	15	9	6	-7	16
Movement happened	Movement happened	-166	46	-32	-33	17

Table 6. Correlation coefficient of rainfall characteristics with horizontal and vertical displacement of points of observation in 7 time intervals

Movement	Whole duration of rainfall	Average of duration of rainfall	Snow height	Amount of rainfall	Average of intensity of rainfall	Intensity of rainfall in different time interval(mm/hr)			
						10	20	30	60
Vertical	0.006	0.02	0.018	0.006	0.029	0.62	0.40	0.38	0.43
Horizontal	0.092	0.118	0.103	0.060	0.864	0.37	0.60	0.66	0.53

List of Figures

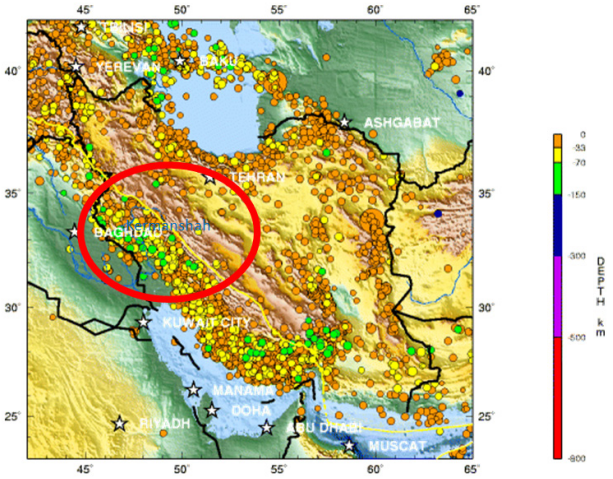

Figure 1. Study area and the location of Kermanshah

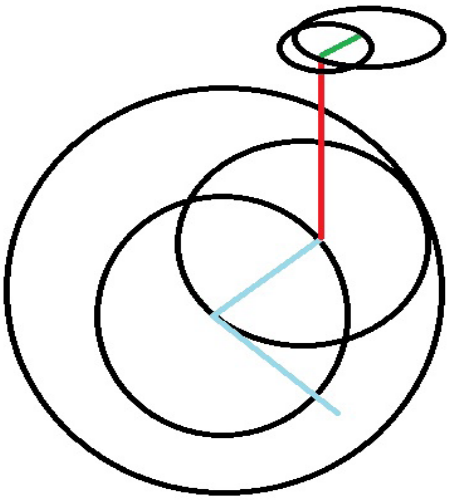

Figure 2. The minimum displacement vector of the points of observation with its opaque error on a part of the area

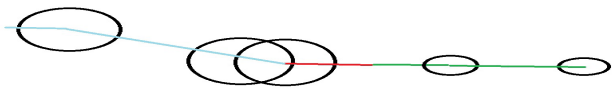

Figure 3. The maximum displacement vector of the points of observation with its opaque error on a part of the area

DOI: https://doi.org/10.30564/jgr.v2i4.1818

References

[1] Alcántara-Ayala, I., Sassa, K., Mikoš, M., Han, Q., Rhyner, J., Takara, K., Nishikawa, S., Rouhban, B., Briceño, S.. The 4th world landslide forum: landslide research and risk reduction for advancing the culture of living with natural hazards. International Journal of Disaster Risk Science, 2017, 8(4): 498-502.
DOI: https://link.springer.com/article/10.1007/s13753-017-0139-4

[2] Bordoni, M., Meisina, C., Valentino, R., Lu, N., Bittelli, M., Chersich, S.. Hydrological factors affecting rainfall-induced shallow landslides: from the field monitoring to a simplified slope stability analysis. Engineering Geology, 2015, 193: 19-37.
DOI: https://www.sciencedirect.com/science/article/pii/S0013795215001222

[3] Ciabatta, L., Massari, C., Brocca, L., Salciarini, D., Moramarco, T., Wagner, W., Tamagnini, C., April. A satellite-based distributed model for landslide risk assessment. In EGU General Assembly Conference Abstracts, 2018, 20: 8676.
DOI: http://adsabs.harvard.edu/abs/2018EGUGA..20.8676C

[4] Hashemian, A.H., Rezaei, M., Kashefi, H., Pirsaheb, M., Kharajpour, H.. Trend step changes of seasonal and annual precipitation over Kermanshah during a 60-year period using non-parametric methods. Bioscience Biotechnology Research Communications, 2017, 10(4): 662-671.
DOI: http://bbrc.in/bbrc/2018Oct%20-%20DecPDF/BBRC17_008.pdf

[5] Hong, H., Kornejady, A., Soltani, A., Termeh, S.V.R., Liu, J., Zhu, A.X., Ahmad, B.B., Wang, Y.. Landslide susceptibility assessment in the Anfu County, China: comparing different statistical and probabilistic models considering the new topo-hydrological factor (HAND). Earth Science Informatics, 2018, 11(4): 605-622.
DOI: https://link.springer.com/article/10.1007/s12145-018-0352-8

[6] Huang, F.M., Wu, P., Ziggah, Y.Y.. GPS monitoring landslide deformation signal processing using time-series model. International Journal of Signal Processing, Image Processing and Pattern Recognition, 2016, 9(3): 321-332.
https://www.researchgate.net/profile/Yao_Yevenyo_Ziggah/publication/299604868_GPS_Monitoring_Landslide_Deformation_Signal_Processing_using_Time_series_Model/links/5702a7aa08aea09bb1a3014b.pdf

[7] Krkač, M., Špoljarić, D., Bernat, S., Arbanas, S.M.. Method for prediction of landslide movements based on random forests. Landslides, 2017, 14(3): 947-960.
DOI: https://link.springer.com/article/10.1007/s10346-016-0761-z

[8] Lin, M.L., Wu, Y.T., Wang, K.L., Hsieh, Y.M.. Monitoring of the Deep-seated Landslide using MEMS-a Case Study of Lantai Landslide, Taiwan. In EGU General Assembly Conference Abstracts, 2018, 20: 12531.
DOI: http://adsabs.harvard.edu/abs/2018EGUGA..2012531L

[9] Melillo, M., Brunetti, M.T., Peruccacci, S., Gariano, S.L., Guzzetti, F.. Rainfall thresholds for the possible landslide occurrence in Sicily (Southern Italy) based on the automatic reconstruction of rainfall events. Landslides, 2016, 13(1): 165-172.
DOI: https://link.springer.com/article/10.1007/s10346-015-0630-1

[10] Pham, B.T., Bui, D.T., Pham, H.V., Le, H.Q., Prakash, I., Dholakia, M.B.. Landslide hazard assessment using random subspace fuzzy rules based classifier ensemble and probability analysis of rainfall data: a case study at Mu Cang Chai District, Yen Bai Province (Viet Nam). Journal of the Indian Society of Remote Sensing, 2017, 45(4): 673-683.
DOI: https://link.springer.com/article/10.1007/s12524-016-0620-3

[11] Rossi, M., Luciani, S., Valigi, D., Kirschbaum, D., Brunetti, M.T., Peruccacci, S., Guzzetti, F.. Statistical approaches for the definition of landslide rainfall thresholds and their uncertainty using rain gauge and satellite data. Geomorphology, 2017, 285: 16-27.
DOI: https://www.sciencedirect.com/science/article/pii/S0169555X17300855

[12] Setiawan, H., Sassa, K., Takara, K., Miyagi, T., Fukuoka, H.. Initial pore pressure ratio in the earthquake triggered large-scale landslide near Aratozawa Dam in Miyagi Prefecture, Japan. Procedia Earth and Planetary Science, 2016, 16: 61-70.
DOI: https://www.sciencedirect.com/science/article/pii/S1878522016300078

[13] Skofronick-Jackson, G., Huffman, G., Stocker, E., Petersen, W.. Successes with the Global Precipitation Measurement (GPM) Mission. In 2016 IEEE International Geoscience and Remote Sensing Symposium (IGARSS), IEEE, 2016: 3910-3912.
DOI: https://ieeexplore.ieee.org/abstract/document/7730015/

[14] W. Yang, L. Shen, P. Shi. Mapping landslide risk of the world. In World Atlas of Natural Disaster Risk (pp. 57-66). Springer, Berlin, Heidelberg, 2015.
DOI: https://link.springer.com/chapter/10.1007/978-3-662-45430-5_4

DOI: https://doi.org/10.30564/jgr.v2i4.1818

BILINGUAL PUBLISHING CO.
Pioneer of Global Academics Since 1984

Journal of Geographical Research
https://ojs.bilpublishing.com/index.php/jgr

ARTICLE

Application of UAV in Road Safety in Intelligent Areas

Yanan Xu[1, 2] Jianxin Qin[1*] Pengcheng He[2] Zhuan Chen[2]

1. Hunan Key Laboratory of Geospatial Big Data Mining and Application, Hunan Normal University, Changsha, 410081 China
2. School of Surveying and Mapping Engineering, East China University of Technology, Nanchang, 330013, China

ARTICLE INFO

Article history
Received: 26 April 2020
Accepted: 28 April 2020
Published Online: 30 April 2020

Keywords:
UAV
Low-altitude RS technology
Road safety
Road repair
Road detection

ABSTRACT

With the continuous development of remote sensing(RS) technology, the surface information can be collected conveniently and quickly by using the popular unmanned aerial vehicle(UAV). The application of UAV low altitude RS technology in road safety in intelligent area has certain practical significance. It can provide safety warning for most drivers, and provide auxiliary decision-making for the road supervision department. Through the collection, processing, calculation and analysis of the road image, the UAV can find out the road obstacles with potential safety hazards, identify the road pit, calculate the radius and depth of the road pit through the digital mapping system, predict the accident risk according to different speed and provide scientific basis for the road safety monitoring. At the same time, UAV can provide repair scheme for damaged roads, estimate the quantity of materials needed for repair, and achieve the target of resource saving and efficiency improvement. The experimental results show that the UAV can not only provide scientific prediction information for driving safety, but also provide relatively accurate material consumption for road repair.

1. Introduction

With the construction and development of traffic, the total mileage of highway is increasing year by year, the density of highway coverage is increasing grow with each passing day, and the mileage of various grades of highways is gradually expanding [10]. However, the obstacles on the road surface will bring inconvenience and hidden safety risks to the driving vehicles. The common obstacles on the road surface include large cracks, local bulges and potholes. In the process of driving, the driver can easily grasp the cracks and bulges of the road surface visually, so as to detour. But potholes are often hard to detect, according to industry insiders, when the car quickly through the road, the impact strength of the tire will increase. If the force is greater than the original bearing capacity of the tire, it may even cause bubbles or even rupture of the tire, resulting in traffic accidents. In addition, if the car passes through the pit at high speed, it will directly affect the suspension system of the car. In serious cases, the hub may break or even leak oil.

**Corresponding Author:*
Jianxin Qin,
School of Surveying and Mapping Engineering, East China University of Technology, Nanchang, 330013, China;
Email: qjxzxd@sina.com
Funded projects:
National Natural Science Foundation (51708098), Key Laboratory Project of National Bureau of Surveying and Mapping Geographic Information for Watershed Ecology and Geographic Environment Monitoring (WE2016018)

 DOI: https://doi.org/10.30564/jgr.v2i4.1835

If the road pit is too deep, it may even touch the chassis and cause more damage. Therefore, it is very important to check and maintain the road and sidewalk irregularly. In this paper, the UAV low altitude RS technology is used to collect and analyze the road image, and finally the judgment result is obtained, which provides the decision-making basis and auxiliary support for the road management department.

UAV was developed in the early 19th century. In the 1980s, drone technology began to be used in various fields, such as battlefield simulation, target surveillance, geodesy mapping, traffic management, resource detection, and environmental protection [3]. Since the beginning of the 21st century, UAV have matured. Its scope of application is constantly expanding, and has achieved good practical results and application value. Currently, drones have been used in more than 40 countries/regions around the world [4]. However, through literature search, it is found that drones are used less in road safety [8].

At present, various road safety inspections mainly rely on manual patrols to find and handle problematic roads through one-on-one inspections, photos and records, and people's reactions. However, the manual inspection has the following problems: Firstly, due to the large traffic road area, the manual inspection has a large workload and low efficiency. Manual inspection requires a lot of manpower, material and financial resources. Secondly, the diversification of road types and the impact of the surrounding environment of the road will inevitably lead to omissions in the inspection process. Thirdly, manual inspections are affected by subjective factors such as employees 'own qualities and professional skills, which can lead to poor accuracy or omissions. Road maintenance is also carried out by manual and special vehicles. The maintenance materials required for each road maintenance task can only be approximated. There is no relatively accurate reference value [9].

In view of the above situation, if the UAV technology with the advantages of intelligence, high efficiency, short cycle and large range is used instead of the traditional pure manual inspection method, the work efficiency will be greatly improved [12]. It can provide the basis for decision-making for road management in smart areas. Provide warning signals for driving vehicles, reduce unnecessary safety accidents, and provide scientific basis for maintenance work.

2. Research Methods

The main content of this research is to collect, process and identify road images. Through calculation and analysis of abnormal road objects, solutions are proposed respectively to provide scientific and quantitative decision-making basis for road safety guarantee or remediation.

During the research, the hardware mainly includes: the image data collection mainly uses the UAV low-altitude RS technology and the control point positioning uses the handheld GPS technology; the software mainly includes: Global Mapper, Pix4D mapper, ENVI and ArcGIS software. Then, the analysis results are provided to relevant departments in a visual form. The technical route is as follows:

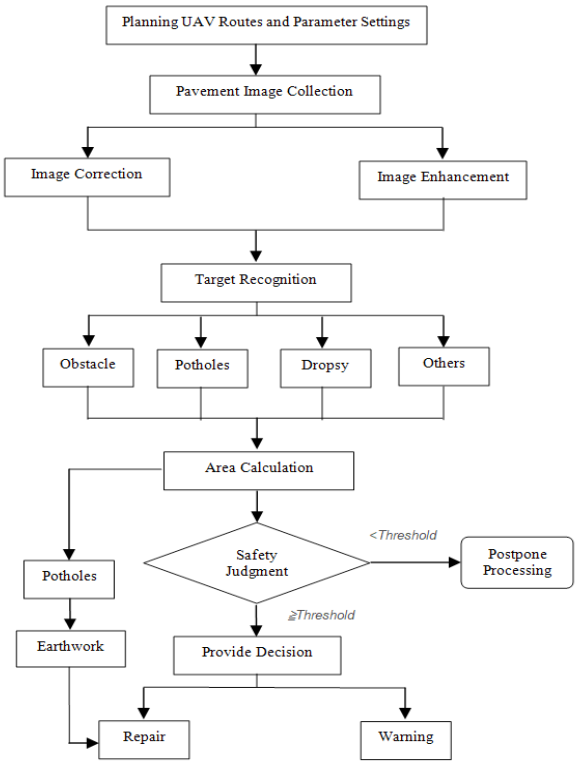

Figure 1. Technical roadmap

3. Research Area and Data Collection

This road safety monitoring data collection area is a Xin-Jian county in Nanchang city, China. Based on the previous Macro-survey of self-driving tours, data collection is divided into two categories. One is an ordinary highway with an average speed of 50 km/h on Xingguo Road and the other is a circular highway with an average speed of 80 km/h at the intersection of Hu-Rui line and Meiling Avenue on Fengsheng Highway.

This paper uses the ground control station software DJI GS PRO that comes with the UAV in Dajiang to plan and control the route. The main parameter settings are shown in Table 1, based on the identified subjects and the data collection range.

DOI: https://doi.org/10.30564/jgr.v2i4.1835

Table 1. UAV parameter setting

Sampling Point Number	Area Location	Flight Mode	Alti-tude (m)	Resolu-tion (px)	Overlap%		Return mode
					Course	Side-by	
Point 1	Xingguo Road	Isochro-nous	60	2.6	70	60	Auto return 10 meters above flight height
Points 2, 3, 4, 5 are on the same road	Intersec-tion of Shang-hai-Rui Line and Meiling Avenue	Isochro-nous	50	2.2	70	60	
		Isochro-nous	80	3.5	70	60	
		Isochro-nous	100	4.3	70	60	
		Hovered	100	4.3	70	60	

The two types of experimental areas were repeatedly photographed by UAV, and the best quality collected data was selected for processing. The orthophotos were processed by Pix 4D software.

4. Image Correction and Enhancement

4.1 Image Registration and Geometric Correction

Due to the error of the UAV image acquisition system itself, multiple orthophotos need to be geo-registered through software to accurately match the geographic location [1]. In this registration, 4 control points are selected on average in the aerial photography area, and the X, Y coordinates and residuals of the control points are set below 0.05 m.

Figure 2. The 1st point area (XingGuo Road)

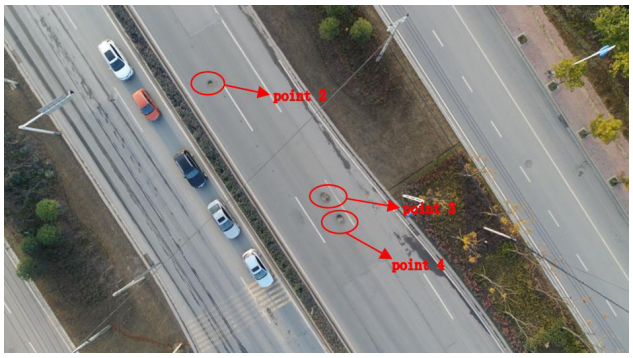

Figure 3. The 2nd&3rd&4th point area (Hu-Rui Line)

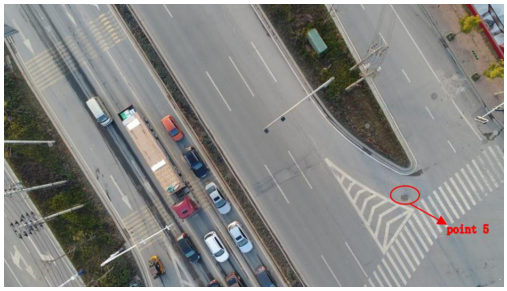

Figure 4. The5th point area (The intersection of Meiling Road and Hu-Rui Line)

4.2 Target Recognition

In order to effectively identify the image content after registration, accurately locate the research object, and identify different targets from the road, in the data collection area, the main road surface abnormalities are divided into obstacles (mainly belonging to things that fall from the moving vehicles), water accumulation (rainwater stored in low-lying areas on the road), and potholes (as a result of long-term rolling, especially the rolling of overloaded vehicles, the depressions on the road surface are pressed deeper and deeper, forming potholes). According to the actual situation in the survey area, obstacles (almost undetected) and accumulated water (the sampling day is sunny) are not considered, so the main research object is road surface depression (referred to as "road pit"). The main task of road pit identification is to determine its boundary. The data after data preprocessing uses RS image processing software (ENVI) to perform target recognition on the image data. The main process is:

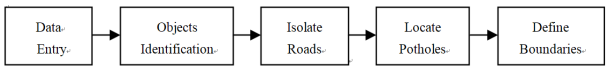

Figure 5. Target recognition process

In the isochronous aerial mode, the boundary between point 1 with an aerial photo height of 60m and point 2-5 with an aerial photo height of 50m is determined as follows:

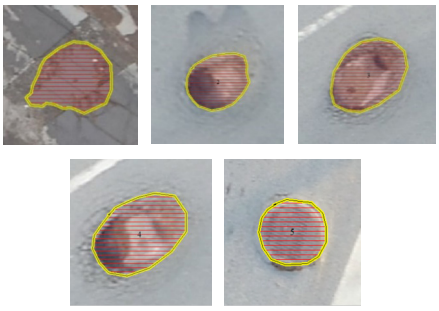

Figure 6. The 1st to 5th point boundary graph

DOI: https://doi.org/10.30564/jgr.v2i4.1835

5. Experimental Results

As mentioned earlier, four different types of flight modes were adopted for points 2-5, namely, isochronous flight height of 50 meters, isochronous flight height of 80 meters, isochronous flight height of 100 meters, and hover height of 100 meters. As a result, it was found that the ground resolution of the isochronous aerial altitude of 50 meters was the highest, which was conducive to data calculation and analysis. Therefore, in the later calculations, points 2-5 used this aerial photography data.

After determining the boundary of the road pit by using ENVI for extracting the abnormal target of the road surface, calculate the perimeter and area of the road pit. The depth of the road pit is temporarily replaced by the average value, and then carefully considered when calculating the amount of earthwork in the later period. The calculation data is as follows:

Table 2. The Calculation results of 1st to 5th points data (Unit: m/m^2)

ID	Circumference	Area	Average elevation of road pit Center	Average elevation of surrounding ground	Road pit depth
1	8.05	4.33	39.33	39.47	0.14
2	2.12	0.33	22.66	22.78	0.12
3	3.51	0.91	22.02	22.12	0.10
4	3.30	0.77	22.00	22.09	0.09
5	3.43	0.87	19.89	19.96	0.07

6. Application of Results

According to the research technical route, it mainly analyzes from two aspects of safety warning and road repair. The calculation results should provide people with quantitative and scientific basis, and display it in an intuitive way, which is convenient for later treatment and prevention.

6.1 Safety Alert

For the pavement with pit, the road safety is analyzed from two aspects of speed and pit size, and the vehicle size and performance are not considered temporarily.

First factor: Speed

In the process of road driving, the higher the speed, the greater the risk of traffic accidents. According to the research of relevant departments in Australia, when the vehicle speed exceeds 60km/h, the risk of traffic accident for every 5km/h increase in vehicle speed is basically twice that of the original. Therefore, when the vehicle is running at a higher speed, small speed changes will have a very obvious impact on driving safety.

The relationship between vehicle speed and the risk of traffic accidents is based on the risk at a speed of 60km/h (set as 1). The risk after each increase of 5km/h is as follows:

Table 3. Relationship between risk index and vehicle speed

vehicle speed (km/h)	60	65	70	75	80	85
Risk Index	1.00	2.00	4.16	10.60	31.81	56.55

Second factor: Road pit size

First of all, the radius of the pit should be accurately calculated, and then the risk analysis should be carried out. Through the target recognition of the image, it is found that the shape of the pavement potholes is approximately circular. In the analysis process, the radius is approximately taken as the model parameter.

Accurate calculation of road pit radius, the author believes that there are two methods, ring average algorithm and ray average method.

(1) Ring average algorithm. For irregular road pit polygons, the change range of its radius is usually not too large, but floating within a certain range. At this time, the average value of the maximum and minimum radius can be used to calculate the size of the road pit radius, as shown in the figure.

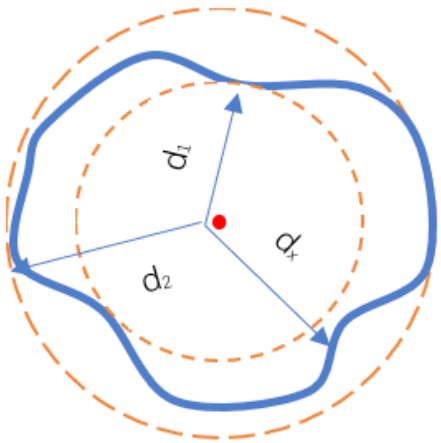

Figure 7. The radius of the ring mean value algorithm

The solid line outline represents the actual road pit polygon, and the two dashed lines inside and outside refer to the ring formed by the minimum inscribed circle radius and the maximum circumscribed circle radius. Then the average radius is: $d_x = (d_1 + d_2) / 2$

DOI: https://doi.org/10.30564/jgr.v2i4.1835

Table 4. The calculation radius and error of the ring mean value algorithm (unit: m/m^2)

ID	Circumfer-ence	Area	Backcalcula-tion radius	Inner tan-gent circle radius	Circum-scribed cir-cle radius	Mean radi-us	error
1	8.05	4.33	1.23	0.75	1.51	1.13	0.10
2	2.12	0.33	0.33	0.24	0.40	0.32	0.01
3	3.51	0.91	0.55	0.43	0.63	0.53	0.02
4	3.30	0.77	0.51	0.37	0.57	0.47	0.04
5	3.12	0.79	0.50	0.49	0.50	0.50	0.00

The above theoretical calculation radius is the average value of the radius inversely calculated by the perimeter and area, and the average radius is the average value of the radius of the inscribed circle and the radius of the circumscribed circle. According to the calculation results and field investigation, the radius difference between the back calculation radius algorithm of point 1 and the ring average algorithm is 10cm, which is relatively large. The reason is that this is a large road pit formed by long-term rolling of vehicles. The larger the pit is, the greater the impact on the surrounding subgrade is. Finally, the irregular area is formed. The closer the polygon is to the circle, the smaller the error of this method is. Otherwise, the greater the error is Like the area of point 1; point 2, 3 and 4 are approximate to the circle, so the ring average algorithm is approximate to the radius of back calculation; the error of two calculation results of point 5 is 0, because here is a well cover, and the surrounding area of the well cover is higher than here due to road renovation, forming a low-lying well cover.

(2) Feature ray average algorithm. The characteristic ray is made from the center of the road pit to the edge of the surrounding pit. The so-called characteristic ray is to find the characteristic point (the point with great curvature change) on the polygonal boundary line, and the line from the center to the characteristic point is the characteristic ray. The sum of all characteristic ray lengths is divided by the number of rays, and the value is the approximate size of the variable pit radius, as shown in the figure:

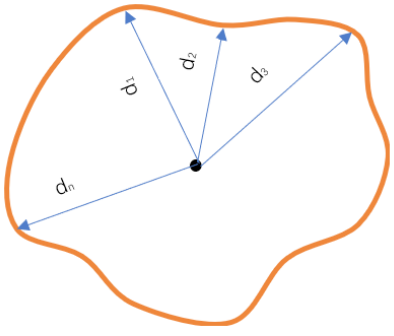

Figure 8. The radius of the characteristic ray averaging algorithm

Road pit radius:$d_x=(d_1+d_2+d_3+\ldots\ldots+d_n)/n=\sum_{i=1}^{n} di/n$. .

Table 5. The calculation radius and error of characteristic ray averaging algorithm(unit: m)

ID	Backcalcula-tion radius	radius of character-istic ray 1	radius of character-istic ray 2	radius of character-istic ray 3	radius of character-istic ray 4	radius of character-istic ray 5	Mean radi-us	error
1	1.23	1.45	1.37	1.19	1.24	1.21	1.29	0.06
2	0.33	0.28	0.41	0.27	0.33	0.29	0.32	0.01
3	0.55	0.68	0.51	0.54	0.48	0.45	0.53	0.02
4	0.51	0.43	0.44	0.58	0.39	0.46	0.46	0.05
5	0.50	0.49	0.50	0.51	0.53	0.48	0.50	0.00

The principle of feature ray selection is to find out the feature points with great changes along the road pit boundary. Connecting this point to the road pit center is the feature curve. The above five feature rays are taken for calculation. The calculation results are not difficult to find, the error of point 1 is still large, the error of points 2, 3 and 4 is small, and the error of point 5 is still 0, because the well cover area here is approximately round, and the feature points have little change.

As mentioned above, the danger coefficient of driving has an exponential relationship with the speed of the vehicle, and the danger coefficient of driving has a regional linear relationship with the radius of the road pit. Therefore, in the case of bad road conditions, especially multi-pit roads, the driving hazard coefficient, vehicle speed and road pit size are in line with the binary nonlinear regression analysis model, and it is increasing.

The functional relationship between the risk factor and vehicle speed and road pit radius is expressed as:

$W=W_1(v)+W_2(d)$

Here's a hypothesis based on the facts:

(1) When $0<d<2/3$ r:W_2 is approximately equal to 0, when the pit radius is less than two-thirds of the wheel radius, it is considered safe and can be decelerated through;

(2) When $2/3r<d<r$:W_2 increases rapidly with d, it should be especially cautious and avoid passing.

(3) When $d > 2r$: W_2 decreases with d increasing, that is, the size of the road pit is much larger than the size of the wheel, if there is no water in the road pit, it can slow down the passage.

For an example of a general domestic car, the tire radius = tire width×aspect ratio+inner radius×25.4 (mm).The letter 195/65R15 is marked on the tire of the Ford car that the author drives, so the tire radius = 195×0.65+15×25.4/2=317.3mm. Comparing with the five collecting points, give some reference traffic opinions.

DOI: https://doi.org/10.30564/jgr.v2i4.1835

Table 6. Reference of vehicle passing through the pit (The tyre radius is 0.32m)

ID	Radius of road pit calculated by characteristic ray method	Wheel comparison	Opinions about passage
1	1.29	>2r	If there is no water in the pit, you can slow down the passage
2	0.32	2/3r<d<r	Slow down for passage
3	0.53	0<d<r2/3	Please avoid
4	0.46	0<d<r2/3	Please avoid
5	0.50	0<d<r2/3	Please avoid

Based on this analysis result, data updates can be made with traffic broadcasting, electronic maps or navigation software to promptly alert car owners to avoid accidents.

6.2 Road Repair

The key to effectively solve the pavement repair is to know the degree of road damage in advance, and then calculate the required materials. This paper excludes other road damage, in terms of pit repair, the solution is based on the collected data. Since the general shape of the road pit is similar to that of a cone, the calculation of the amount of soil in the road pit is expressed as:

$V=S\times h/3$

V is the amount of soil in the road pit, S is the area of the pit, h is the depth of the pit.

Of course, the general road pit is not a regular cone, that is, the road pit is not a fixed value. Here we can only estimate roughly. If you need to calculate the amount of earth carefully, you can use the calculating method to calculate the volume capacity of the pit. Based on road construction experience, materials are often prepared 1.3 times the amount of earth calculated, according to $V=1.3(V_1+V_2+...V_n)$. Prepare for reasonable allocation of manpower, resources and time. In this paper, the list of soil quantity of road pits in the experimental image collection is as follows:

Table 7. Calculation results of earthwork of points (unit: m^3)

ID	Area	Road pit depth	Earthwork volume
1	4.33	0.14	0.20
2	0.33	0.12	0.01
3	0.91	0.10	0.03
4	0.77	0.09	0.02
5	0.87	0.07	0.02

For the study area, the total soil volume of the five road pits collected is:

$V=1.3*(V_1+V_2+V_3+V_4+V_5=0.20+0.01+0.03+0.02+0.02)=0.364m^3$

When this data is fed back to the municipal or road management departments, it is targeted at repairing the road pit before preparing 0.364 m^3 materials. This not only makes the quantification scientific, avoids waste of materials, but also improves the work efficiency.

As mentioned above, whether it is safety warning or road repair, it is feasible to use UAV low-altitude remote sensing technology. If the scope is widened and the processed data is reported to the transportation department and the government department in time, it has certain practical significance to prevent traffic accidents and scientific road repair.

7. Conclusion

Through the low-altitude RS technology of the UAV, collecting road images, after processing and analysis, will greatly improve the efficiency of road detection, reduce costs of road maintenance and road safety and maintenance ,and bring convenience to actual production and life. Successful studies in this area are as follows:

(1) It is economical and practical to use UAV technology to collect road image data. Taking full advantage of UAV can collect data conveniently and quickly, reduce cost and improve efficiency.

(2) It is reliable and feasible to process image data through professional RS and GIS software. All the data are processed by mature software, the process is not affected by human factors, and the data obtained is consistent with the actual situation.

(3) The method of geographic mathematical modeling is used for analysis and judgment, which is both accurate and precise. In-depth mining of the collected data to establish a judgment model to provide accurate and precise judgment results, so it can withstand practical tests.

(4) It can provide decision-making basis for road management department through visual expression, which is easy to read and understand. The visual expression allows road managers and users to see the research results at a glance, quickly assist decision-making, and make timely responses to reduce accidents and property losses caused by hidden road safety hazards.

References

[1] Xinteng Li, Xiaoyong Chen, Teng Gu, etc.. Comparison of image fusion methods between High Score 1 and Land sat 8[J]. Journal of East China University of Technology (Natural Science Edition), 2017, 40(04): 376-380.

[2] Zhong Cao. Current status and prospects of low altitude unmanned aerial vehicle forest resource investigation and monitoring application[J]. Forestry

DOI: https://doi.org/10.30564/jgr.v2i4.1835

construction, 2016(06): 1-5.
[3] Qiang Chen. Research on traffic accident scene survey technology based on real-virtual target fusion and UAV photography[D]. Jilin University, 2017.
[4] Deren Li, Ming Li. Research progress and application prospects of unmanned aerial vehicle remote sensing system[J]. Journal of Wuhan University (Information Science Edition), 2014, 39 (05): 505-513+540.
[5] Fengxian Li. Application and discussion of UAV technology in remote sensing monitoring of grassland ecology[J]. Survey and Mapping Notice, 2017(07): 99-102+107.
[6] Mingbo Li, Ping Chen, Zhihua Chen. Study on the Key Factors of Rainfall Landslide Disasters in Hunan Province[J]. Journal of East China University of Technology (Natural Science Edition), 2018, 41(01): 36-40.
[7] Luheng, Li Yongshu, He Jing, etc. Acquisition and processing of low-altitude remote sensing image data of unmanned aerial vehicle[J]. Surveying and Mapping Engineering, 2011, 20(01): 51-54.
[8] Zezhong Ma, Fuhai Wang, etc. Application of low-altitude unmanned aerial vehicle remote sensing technology in monitoring landslide and weir Lake disasters in Chengkou, Chongqing[J]. Journal of Soil and Water Conservation, 2011, 25(01): 253-256.
[9] Xinlu Nie, Fei Tang, Qianhong Zhu. Application of UAV remote sensing technology in urban rail transit inspection[J]. Modern urban rail transit, 2017(10): 58-61.
[10] Yifan Pan, Xianfeng Zhang, Child Jubilee, etc. Progress in remote sensing monitoring of highway pavement quality[J]. Journal of Remote Sensing, 2017, 21(05): 796-811.
[11] Guanling Zhang. Application of UAV low altitude photogrammetric system[J]. Engineering technology research, 2017(04): 24+110.
[12] Zhiwei Zhang. Study on monitoring system of straw burning based on low-altitude remote sensing technology[J]. Hubei Agricultural Science, 2016, 55(02): 481-485+500.

 DOI: https://doi.org/10.30564/jgr.v2i4.1835

BILINGUAL PUBLISHING CO.
Pioneer of Global Academics Since 1984

Journal of Geographical Research
https://ojs.bilpublishing.com/index.php/jgr

ARTICLE

The Dynamics Mechanism of Vulnerability for Resource-based Enterprise Communities in China

Lichun Hou[1,2] Zhenshan Lin[2*] Ping Wang[3*] Fanyuan Zeng[1] Chao Han[4]

1. Shangrao Normal University, Shangrao, 334000, China
2. School of Geographical Science, Nanjing Normal University, Nanjing, 210000, China
3. Hainan Tropical Ocean University, Sanya, 572002, China
4. Linköping University, SE-58183 Linköping, Sweden

ARTICLE INFO

Article history
Received: 8 May 2020
Accepted: 18 May 2020
Published Online: 31 May 2020

Keywords:
Resource-based enterprise community
Vulnerability
Large enterprise
Nonlinear
Dynamics

ABSTRACT

This paper has analyzed the dynamics mechanism of resource enterprises community vulnerability, selected the key factor of resources to establish a nonlinear dynamical model. The model reveals the constrained relationship between the number of vulnerable enterprises and resource shortage rate, and the same relationship between t vulnerable enterprise numbers and the owning rate of resource market by the biggest enterprise in resource-type enterprises community of China. The results showed that, the shortage rate of resources take up more percentage than the occupancy of resource rate of the strongest enterprises in Enterprise community when D>q. the characteristics and patterns of the Chinese enterprise evolution are as follows, (1) The strongest enterprises n1 will decline or transform in the enterprise community. (2) The enterprises which survived after the shortage of resources will go through three stages: ① resistance stage; ② recovery stage; ③ stable stage. We believe that there are three movements that can make sure the resource-based enterprises community keep growing continuously in the competitive market for resources, (1) understand the enterprise resources shortage rate and the strongest enterprises share in resource rate in enterprise community, (2) follow the even-odd symmetry or odd-even symmetry laws based on the familiarity of a resource economy, (3) put the enterprises in the suitable position.

1. Introduction

In the process of economic globalization, the globalization of resources allocation and integration of international market are gradually becoming more significant, meanwhile, in a global scale, the adjustment and upgrading of industrial structure are having a rapid pace, it is also noticeable that the mergers of large enterprises and companies goes hand in hand with the rise of a large number of small and medium-sized enterprise communities. Particularly noticeable [1]. The Ministry of land and resources survey shows that, by the end of 2002, 2/3

**Corresponding Author:*
Zhenshan Lin,
School of Geographical Science, Nanjing Normal University, Nanjing, 210000, China;
Email: Linzhenshan@njnu.edu.cn;
Ping Wang,
Hainan Tropical Ocean University, Sanya, 572002, China;
Email: wangpingalong@163.com

DOI: https://doi.org/10.30564/jgr.v2i4.1871

of large and medium-sized state-owned resource-based enterprises are facing depletion issues in China [2]. By the October of 2012, 5010 state-owned large-medium-sized enterprises and mines with exhausted resources in China have exited the market [3]. These symptoms are the comprehensive reflection of resource-based enterprises community vulnerability [4]. Since 1980s, Chinese government has started to assign large amounts of funds to support state-owned resource-based enterprises, trying to promote the development of other alternative industries, so that they are able to complete industry transformation successfully before the exhaustion of resources [5-8]. This paper considers that the resource-based enterprises community is the base for the survival of enterprises, formed by gathering some enterprises related to mining, processing and utilization in certain areas, and provide resources and primary processing products to society, with the features of opening, dynamic, nonlinear, complex adaptive etc. The vulnerability [9] refers to the character of resource-based enterprises community breakdown due to the depletion of resources, which can cause an enterprise with more instability, sensitivity and lack of recovery ability. In short, the vulnerability is the root of the resource-based enterprises community decline. When resource based enterprise confronted the resource constraint for some reason, vulnerability will become more obvious. Therefore, the resources are the largest contributors for community development [10]. Therefore, resources are selected as the key factor to prove.

The resources shortage will lead to the decline or transformation of some enterprises, but how the resources shortage affects and restricts mechanism of industrial economy and regional economy of China has not yet been understood profoundly, especially the new pattern of internal mechanism. The lacking knowledge of this area have led to the decline of part of industry and enterprise in China. Although there has been a lot of researches in this area [11-13], but it does not involve inherent dynamical mechanism in between. As the (nonlinear) mathematical difficulties, the relationship between mathematical constraints and dynamic mechanism so far has not been studied by resources economist of China. And this mathematical difficulty mainly due to resource market economic system is a very complex nonlinear system. With the development of nonlinear science and mathematics, quantitative research and dynamics mechanism research have been deep into the earth science, environmental science, resource science and economics etc [14-17]. Only a profound understanding of the intrinsic dynamic relationship and the development mechanism between management object (element) can enable the implementation of scientific and effective government management and reform, so as to achieve the maximum the utilization of limited resources. Therefore, it is necessary to study the intrinsic relationship between the shortage of resources and enterprise decline from the angle of nonlinear dynamics.

From the dynamic perspective, this paper will analyze the dynamic mechanism of vulnerability production of resource-based enterprises community, select the key factor as resources, set up a nonlinear dynamic model of enterprise competition for the first time in describing the enterprise community economy resource market evolution (development or recession), and using this model simulation studies the dynamic constraints relationship on a certain resources shortage rate that will cause Chinese enterprise decline , thus in the competition strength and the competition advantage of the asymmetric conditions, provide scientific theoretical basis with minimal resources shortage rate for the resource-based enterprises community development and positioning, the government and industry departments to study and formulate the governance model for the vulnerability of Chinese enterprise community *(community, population, and the dominant species in this paper refers to the resource type)* .

2. The Resource-based Enterprises Community Competition Dynamics Model

Assuming the total resources is 1 in one certain industry in China, $\mathbf{p_i}$ is the resources occupancy rate(0‹pi‹1) which an enterprise (company) i hold on the resources rate under the resources market economy system; $\mathbf{c_1}$ is resources occupation rate for the enterprise (company) i to peer (population) other enterprise (company) , namely, resource development capacity; $\mathbf{m_i}$ for enterprise i internal rate of decline; D is the resources shortage rate of China under the global resources market economy system.

The so-called enterprise decline under the global resources market economy system, in fact it is that enterprises share of resources Pi with time evolution problem when shortage of certain rate of resources. If Pi tends to zero with time increases and it means that the declining trend of the enterprise. Conversely, if the Pi tends to large with time increases, it means that the enterprise development and expansion.

Because the enterprise (company) share resources rate relate to its competition ability and internal decline rate. Zhenshan Lin put forward the following hypothesis relevant enterprise decline rate m_i and the company share of domestic resources rate ($p_i^0 (i = 1,2 \ldots n)$) when there is no shortage of resources. Hypothesis: each enterprise of peer (a group) has equal internal rate of decline, enterprises (a group) in China as no shortage of resources share on

 DOI: https://doi.org/10.30564/jgr.v2i4.1871

the rate of domestic resources p_i^0 for the geometric series distribution;

$$m_i = m \ \ p_i\big|_{D=0} = q(1-q)^{i-1} \tag{1}$$

In the condition of no shortage of resources, stronger (large) companies have more share on the rate of resources.

Based on the above assumptions, we reference the dynamics model of metapopulation, the following dynamics model of competitive enterprise is proposed under resources market economy:

$$\frac{dp_i}{dt} = c_i p_i (1 - D - \sum_{j=1}^{i} p_j) - m_i p_i - \sum_{j=1}^{i-1} p_i c_j p_j \quad (i = 1,2 \ldots n) \tag{2}$$

Equation (2) illustrates the resources under the market economy system, enterprises in different countries (company) are the coexistence of the resources and the natural decline rate for dynamic balance between competitive ability, exploring different between enterprises, and this balance requires less competitive (small) firms with strong resources development ability. The right side sectors of Equation (2) means the enterprise resources on the successful occupation; enterprise nature (internal) rate decline due to the reduction of resource share; reduction rate of resources possession due to competitive factors.

3. The Dynamic Mechanism of Vulnerability Resource Type Enterprises, When D>q

3.1 Mathematical Derivation and Theoretical Analysis

Assuming that the global resources under the market economy system, the net resources shortage ratio in China is D, Chinese enterprise (a group) survival pattern reach a new equilibrium, enterprise occupies the resource ratio of p_i^e ($dp_i/dt=0$), namely the solution of steady state of (3):

$$p_i^e = \begin{cases} \hat{p}_i & if \quad \hat{p}_i > 0 \quad (\hat{p}_i = 1 - D - \frac{m_i}{c_i} - \sum_{j=1}^{i} p_j^e (1 + \frac{c_j}{c_i})) \\ 0 & if \quad \hat{p}_i \le 0 \end{cases} \quad (i = 1,2 \ldots n) \tag{3}$$

Obviously, $\hat{P}_i \le 0$ false,

$$D \ge 1 - m_i / c_i = 1 - (1-q)^{2i-1} \tag{4}$$

When the condition is met, the top i of strong (large) enterprise (company) in the enterprise population will decline.

The formula (4) is the critical constraint relationship between the decline of large enterprises and the shortage ratio of resources and the strongest (large) enterprise occupies the share of resources.

Figure 1 demonstrates the critical decline constraint conditions of D=1- $(1-q)^{2i-1}$, the relationship between the number of big business enterprise in the decline and resources shortage rate. The graph 5 curves respectively correspond to five kinds of enterprises (companies) situation as q=0.05, 0.1, 0.2, 0.3, 0.4. Wherein, q=0.4 represents the largest enterprise (company) in a certain industry (population) of China have 40% of resources ratio when without shortage of resources. The second companies share of resources $p_2\big|_{D=0} = 0.4(1-0.4)^{2-1} = 0.24$ =24%=24%. Third companies share of resources $p_3\big|_{D=0} = 0.4(1-0.4)^{3-1} = 0.144$ =14.4%,…. While q=0.05 represents the largest enterprise (company) hold 5% of resources rate in a certain industry (population) of China when without the resources shortage. Second big enterprise resource share is $p_2\big|_{D=0} = 0.05(1-0.05)^{2-1} = 0.0475 = 4.75\%$. Third enterprise resource share is $p_3\big|_{D=0} = 0.05(1-0.05)^{3-1} = 4.5\%$,….As you can see from Figure1., the bigger the q, namely stronger the largest enterprise in the enterprise community, lead to less the number of the decline of the enterprise (company) when the shortage of resources, that is weak (small) business are more not easy to decline.

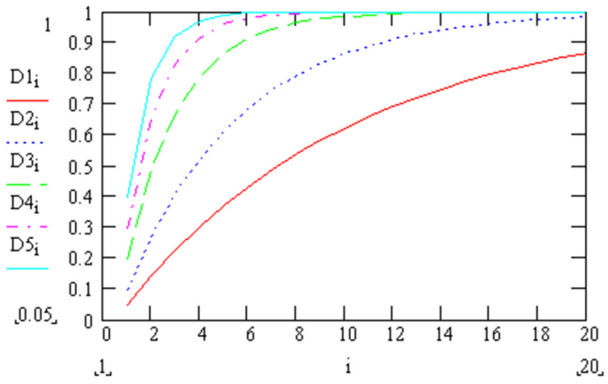

Figure 1. The relationship between enterprise decline and resource shortage rate in the critical decline constraint conditions of D=1-$(1-q)^{2i-1}$, The 5 curves correspond to the q=0.05,0.1,0.2,0.3,0.4, five kinds distribution structure of enterprises

Figure 2 demonstrates the relationship between the number of decline enterprise in community and the strongest (large) enterprise share of resources when in the critical decline constraint conditions of q=1-$(1-D)^{1/(2i-1)}$. The graph 5 curves respectively correspond to the five kinds of resources shortage as D=0.5, 0.4, 0.3, 0.2, 0.1. As you can see from Figure 2: (1) the bigger the q, namely the stronger the largest enterprise in the enterprise community, when the shortage of resources, the less the number of enterprises decline, that is weak (small) firms are less likely to be swallowed up by; (2) The smaller the D, the fewer number of enterprises lead to the decline under global resources market economy.

DOI: https://doi.org/10.30564/jgr.v2i4.1871

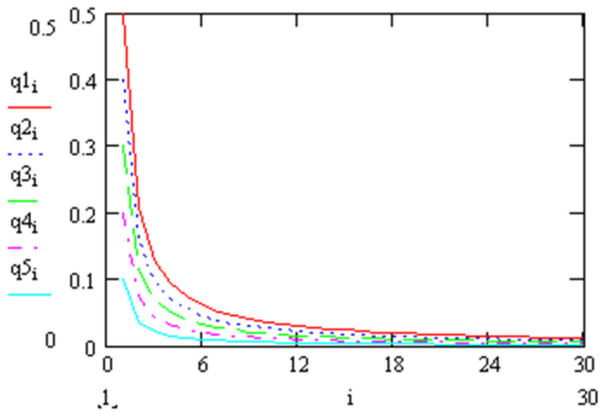

Figure 2. The relationship between the number of enterprise decline and share of resources strongest enterprise, In the critical decline constraint conditions of q=1-(1-D)1/(2i-1). The 5 curves correspond to D=0.5, 0.4, 0.3, 0.2, 0.1 the five cases

Table 1 reveals the relationship between enterprise decline number N and q, with the different resources shortage rate. Table 1 reveals that the strongest (largest) domestic enterprises play a certain protective role on the domestic weak enterprises, under the shortage of resources rate in the global resources market economy. As long as the strongest (large) business does not decline, other enterprises will not be decline because of resource rate shocks (note this theory is only suitable for the case of q<D. The situation of small enterprise first declines will be studied on another paper).

Table 1. The relationship between the number n of enterprise decline and q in shortage rate of resources

	D=0.5	D=0.4	D=0.3	D=0.2	D=0.1
n=1	0.5	0.4	0.3	0.2	0.1
n=2	0.206	0.157	0.112	0.072	0.035
n=3	0.129	0.097	0.069	0.44	0.021
n=4	0.094	0.07	0.05	0.031	0.015
n=5	0.074	0.055	0.039	0.02	0.012
n=6	0.061	0.045	0.032	0.02	0.00953
n=7	0.052	0.039	0.027	0.017	0.00807
n=8	0.045	0.033	0.023	0.015	0.007
n=9	0.04	0.03	0.021	0.013	0.00618
n=10	0.036	0.027	0.019	0.012	0.00554
n=11	0.032	0.024	0.017	0.011	0.0050
n=12	0.03	0.022	0.0145	0.00966	0.00457
n=13	0.027	0.020	0.014	0.00889	0.00421
n=14	0.025	0.019	0.013	0.00823	0.00363
n=15	0.024	0.017	0.012	0.00767	0.00363
n=16	0.022	0.016	0.011	0.00717	0.00339

Table 2 gives the different Q values, the relationship between the shortage of natural resources and enterprise decline number n. Table 2 shows that the maximum enterprise n1 is weak (Q =0.05 small), and smaller shortage rate of D=q=0.05, it will lead to decay or transform; but n2, n3, n4 resistance is nonlinear increase in turn. When D increases to 6 times, n4 will decline. While q is large, n3, n4...etc. almost will not deteriorate in the condition of the shortage of resources. This means, under these conditions, that the small enterprises "adapt" to the changes of resources and environment actively, and It has the potentiality to develop into new large enterprises (the theory is only suitable for the case of q<D. Small enterprise first decline will be another paper).

It is necessary to point out that, the relevant conclusion shows one-sidedness from Table 1 and Table 2 In the future research, we will reveal that the shortage of resources lead to decline of the small business in enterprise community.

Table 2. When different q values, the relationship between resources shortage rate and enterprise decline number n.

	q=0.05	q=0.1	q=0.2	q=0.3	q=0.4
n=1	**0.05**	**0.1**	**0.2**	**0.3**	**0.4**
n=2	**0.143**	**0.271**	**0.488**	0.657	0.784
n=3	**0.226**	**0.41**	0.672	0.832	0.922
n=4	**0.302**	0.522	0.79	0.918	0.972
n=5	**0.37**	0.613	0.866	0.96	0.99
n=6	**0.431**	0.686	0.914	0.98	0.996
n=7	**0.487**	0.746	0.945	0.99	0.999
n=8	0.537	0.794	0.965	0.995	1
n=9	0.582	0.833	0.977	0.998	1
n=10	0.623	0.865	0.986	0.999	1
n=11	0.659	0.891	0.991	0.999	1
n=12	0.693	0.911	0.994	1	1
n=13	0.723	0.928	0.996	1	1
n=14	0.75	0.942	0.998	1	1
n=15	0.774	0.953	0.998	1	1
n=16	0.796	0.962	0.999	1	1

3.2 Dynamic Simulation

Dynamics simulation of Fig.3 reveals that the domestic Enterprises (enterprise community) have dynamics characteristics in the condition of large enterprises decay (D > q) change: (1) the D=0.3 is much greater than q=0.03, namely the resource shortage rate is relatively larger, the strongest enterprises in the domestic Enterprise Inc (enterprise community) will inevitably decline, transform or even conduct mergers and acquisitions of overseas resources. The relaxation time of the strongest enterprise n1 declining is about 220 -1800 months. (2) With the decline of strongest enterprises, the order to the critical threshold of the enterprises were second, third, fourth, fifth strongest enterprises, when D>q, the strong enterprises of China's will decay before the weak enterprises. (3) on the condition of high rate resources shortage, the survival firms will experience the following stages of development and adaptation: ① forced adaptation

DOI: https://doi.org/10.30564/jgr.v2i4.1871

or resistance stage: in the short time period after the shortage of resources (1/m), the share of resources of all enterprises fell sharply. But the weakest companies declined minimally, namely the smallest enterprise in the resource-based enterprises community has the strongest resistance. ② The recovery stage: This is the nonlinear interaction process on a very complex resource type enterprises competition, the concrete manifestation is: Chinese enterprises community within the multi equilibrium coexistence and the strongest enterprises constantly replaced, usually according to the weakest, the second weakest... Order to serve as the strongest enterprises. The recovery phase clearly reveals the local strong enterprises (dominant) are frequently established and alternated. This indicates the resource competition is very fierce; all the surviving enterprise share resource rate changes are periodic in a long period of time. ③ the stable stage: after a long term development, when the system reaches the new equilibrium state, the original top 5 enterprises are orderly decline after the fall, n6, n8, n10 (note not n7!) become the strongest, second strongest and the third strongest enterprises.

We believe that, when the resources shortage ratio D is greater than a certain threshold, the first decline is the most competitive enterprise instead of the weak enterprise that generally thought, the implication behind are as follows: (1) from a perspective of competition mechanism between enterprises within the community, the ability of exploiting resources of strong enterprises is insufficient, and the weak enterprises can survive the condition with resources shortage, because they have strong resources development ability; (2) From the perspective of company stability, the weaker the enterprise to the impact of external resistance, the stronger with its recovery (adaptation) force; on the contrary, the stronger enterprises, the weaker its ability to adapt and recover. Since any strong (large) companies have limited resistance to resource degradation, once the resource changes (shortage) exceeds the limit , the self-adjustment ability will decline rapidly and even disappear, resulting in the strong business decline and transformation. Small businesses have strong recovery ability, so they can quickly adapt to the new situation of resources from resources challenges.

Figure 3(b) clearly shows that Chinese resource-based enterprises community in the recovery stage that excessive state small enterprises played a process of the strongest enterprises from weak to strong by the order (the most dominant species, the strength of possession resources rate are more than the original n1 0.037!) So, Chinese enterprises adaptive development is the revolutionary after the shortage of resources (the cost is the top 5 strong enterprises closed and recession), in the direction of the good (strong). The originally strongest enterprise n1 occupy resources rate of 0.037, while the share of resources rate of n9, n8, n7, n6 are respectively 0.0543 (0.038/0.7), 0.057 (0.040/0.7), 0.06 (0.042/0.7) and 0.063 (0.044/0.7) in the development process; and are respectively 146.8%, 154.1%, 162.2%, 170.3% correspond to the original maximum enterprise resource possessed rate 0.037. Visibly, the ecological system of Chinese enterprises under the global resources market economy is more centralized and monopolized. It may be enough to cope with the new possible competition for resources, the ability of enterprise community against resources shortage has been greatly improved. From Figure 3 (b) can also see that the minimum n10 under natural resources shortage (under the global resources market economy) in 10 years later, n9 in 18 years, n8 in 30 years, N7 in 35 years, n6 in 70 years, respectively become the strongest enterprise of system process; But the strongest is the n6 survivors of final stable Chinese some industries and enterprises system. The enterprise strength order of new equilibrium state is n6-n8-n10 (even) -n7-n9 (odd); namely, the surviving even enterprise will become strong enterprises, and the survived odd enterprises will become the weak enterprises. This is an important symmetry law of business strength order distribution, the following will further study.

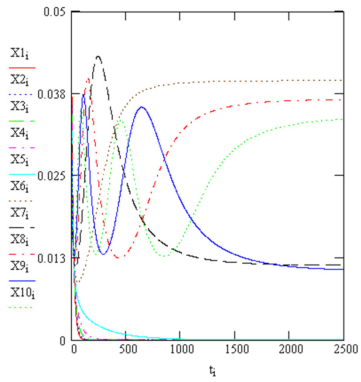

(a)

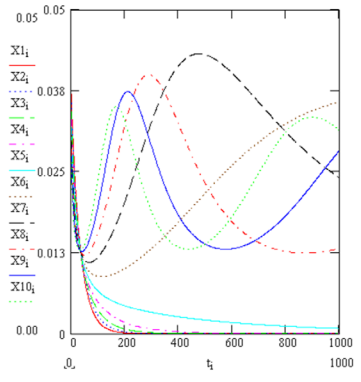

(b)

Figure 3. The relatively large shortage rate causes the decline of top 5 businesses in a resource-based enterprises community of China. The parameters : D=0.3, q=0.037,

DOI: https://doi.org/10.30564/jgr.v2i4.1871

m=0.1, n=10. (a),(b)respectively correspond to different time intervals

The parameters difference in Figure 4 and Figure 3 only lies in the enterprise internal different decay rate. Figure 4 m=0.2, while figure 3 m=0.1. The difference between the simulation results exhibit only shorten to the relaxation time of decay. m=0.1 (Figure 3), the enterprise decline relaxation time is 220 -1800 months, while m=0.2, the enterprise decline relaxation time is 100-900 months. Comparing Figure 4 and Figure 3 we can investigate that the change of m almost does not affect the peak values of the equilibrium state, but only change the peak time. When m is smaller, the emergence of the peak and equilibrium mutation time is longer; when m becomes larger, occurrence of each peak and equilibrium mutation time shorter. m smaller mean enterprise average life cycle increases, resulting in strong corporate succession time growth. While m becomes larger, means that enterprises average life cycle is shorter, resulting in strong enterprises to shorten the time of succession.

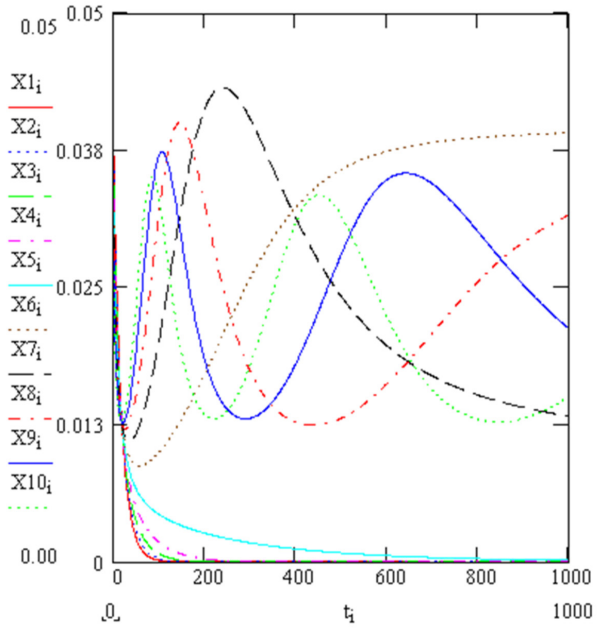

Figure 4. The relatively large shortage rate lead to the decline of top 5 business in a certain industry of China. The parameters: D=0.3, q=0.037, m=0.2, n=10. And the difference with fig.3 (m=0.1) is that shorten the relaxation time of enterprise decline. m=0.1 (Fig.3), 220 -1800 months is enterprise decline relaxation time, m=0.2, enterprise decline relaxation time is 100-900 months

In order to further illustrate the dynamic characteristics and response process of adaptation of enterprise community to the shortage of resources, we are given n=10, D=0.3, and Q respectively 0.1 and 0.15 (corresponding to different industries population structure) of the simulation results, as shown in figure 5a-b.

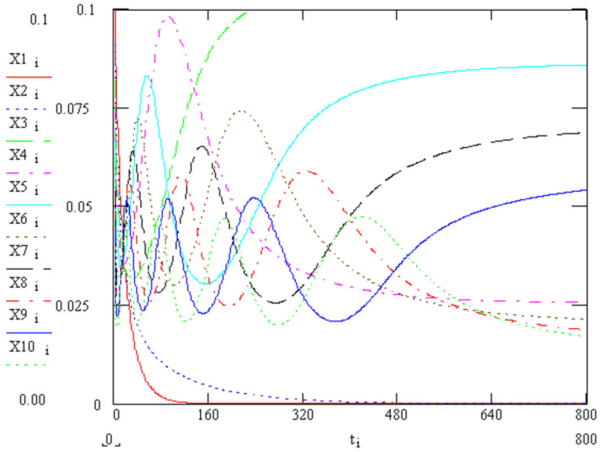

(a)

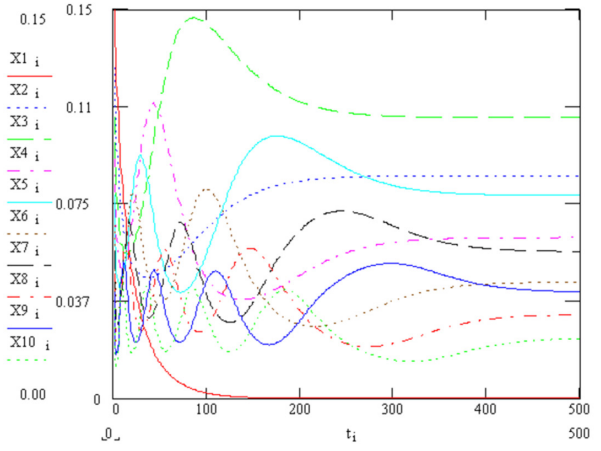

(b)

Figure 5. Response and adaptation process on enterprises for resource shortage. n=10, D=0.3, m=0.02. (a) q=0.1; (b) q=0.15

From figure 5(a-b) and Figure 3 the dates show that: (1) in the premise of D>q, the larger values of D/q, the more the number of the enterprise decline due to the shortage of resources caused by. D/q=0.3/0.037=8 (Figure 3), resource-based enterprises community the top 5 strong enterprises will turn all decay or transformation, and when D/q=0.3/0.15=2 in community only the strongest enterprise N1 decay; (2) After equilibrium coexistence and the strongest enterprises (optimal) continuous replacement process, the ecological system of resource type enterprises achieve new equilibrium state, Chinese (a resource-based industries) enterprises system strength sequence will strictly abide by the even-odd symmetry or odd-even number symmetry laws. It is concluded that if because of the shortage of resources and cause the sys-

DOI: https://doi.org/10.30564/jgr.v2i4.1871

tem to have an odd number of enterprise decline, then after the adaptive stability system (a business) enterprise strength order obey the odd-even symmetry laws, namely the original number-even enterprises become strong, while the original number-odd enterprises turn into the weak. If the community has an number even of enterprise decline, then the enterprise strength order after the adaptive stability system obey the odd-even symmetry laws, namely the original number odd enterprises become strong, while the enterprise for original serial number even into a weak. For example, when D/q=0.3/0.1=3, the top 2 enterprises of the system will decline, then the new equilibrium state enterprises strong weak ordering: n3→n5→n7→n9→n4→n6→n8→n10. And when D/q=0.3/0.15=2, the top 1 enterprises of the system will decline, then the enterprises new equilibrium state strong-weak order: n2→n4→n6→n8→n10→n3→n5→n7→n9.

We believe that under the global resources market economy, different resource type enterprise in China can continue to grow and develop based on following rules, grasping the information of industry resources shortage rate and the resources share of the strong enterprises, recognizing the odd-even symmetry or odd-even symmetry rules under the resources market economic system, and understanding the correct position in business activities.

4. Conclusions

We have used mathematical analysis and numerical simulate and systematically studied the enterprise decay dynamics mechanism and constraint relation for different resource-based enterprise communities in different case of shortage of resources. The results show that in the case of D>q (namely, the rate of resources shortage is greater than the strongest enterprise in the enterprise community share resource rate) and D<q (i.e., the rate of resources shortage is less than the most enterprises in the enterprise community on the rate of resources share), community evolution complies with two distinct dynamics mechanism. In the circumstance of D>q, which refer as resource shortage rate is greater than resource share rate of the strongest enterprise in enterprise community, Chinese enterprises evolution under the global resources market economy has the following rules and characteristics:

(1) The dominant species (strong) enterprise n1 will inevitably decline and undergo transformation in the resource-based enterprises community. With the resource shortage rate increased, the weaker enterprises will decline along with the strongest enterprises. The larger value of D/q comes with more decline of strong enterprise in community. The relaxation time order of magnitude which leads to decline or transit buffer is ranging from 5 to40 years.

(2) When the strongest enterprises n1 is weak in the resource-based enterprises community (q minor), the small disturbance resources (shortage) can cause it to decline and even transform. But the resistance of n2, n3, n4 is increasing nonlinearly in turn. While q is large, n3, n4..... will not decline under the condition of the shortage of resources, which means that the large enterprises in industry system come stronger. When resources shortage appears, the less enterprises decline, and the weak enterprises will not easily decay. This means that small enterprises have become adaptive for the changes of resources environment, which is helpful to further evolve into new large (strong) enterprises at any time.

(3) The surviving enterprises after the resources shortage in the community will experience three stages of evolution: ① The resistance stage: in this stage, the enterprise community (all species) the steeply decline in share resource rate. But the weakest company declined minimally, namely the weakest enterprises in the enterprise community have relatively stronger resistance. ② The recovery stage: This is a complex nonlinear interaction process of many enterprises in various group, except for the n1, all companies in enterprise community have served as the strongest enterprises sequentially according to the weakest, the second weakest... order, showing the frequent establishment and alternation of local area advantage enterprises. China enterprises adaptive evolution is revolutionary evolutions which continuously develop itself in a good way after resources shortage risks. The highly adaptive large enterprises in the community can be more centralized and monopoly sufficient to cope with more potential resources challenges. ③ The stable stage: after multiple equilibria coexist and the strongest enterprises (optimal) continuous replacement process, the enterprise ecological system achieves a new equilibrium state, the system order is strictly abided by the even-odd symmetry or odd-even symmetry law. That is, if because of resources shortage and lead to an odd number of enterprise decline in enterprise community, when it adapted to stability, the community enterprise strength order is following odd-even symmetry rules, namely the enterprises that original serial number for even number will evolve into the strong, and that the original serial number for odd number will evolve into the weak. If there is an even number of enterprises decline in the community, when it becomes stable, the order will obey the odd-even symmetry rules, namely the original odd number of enterprises become strong, and that the original even number evolve into the weak enterprise.

(4) The change of enterprise decline rate m almost does

DOI: https://doi.org/10.30564/jgr.v2i4.1871

not affect the peak value of each equilibrium state of enterprise community; it only changes the peak time. When m comes smaller, the time of the peak emergence and equilibrium mutation become longer; and vice versa.

(5) Whether the declining reason is caused by q or D changes, the dynamic mechanism are the same for large enterprises, the dynamics of changes of q and D is equivalent.

Funding

This work was supported by Jiangxi University Humanities and Social Sciences Research Project of China [No. JC18118], the Humanity and Social Sciences Foundation of Ministry of Education of China (17YJAZH113), Hainan Provincial Natural Science Foundation of China [Grant No.417151], the Doctoral Scientific Research Foundation of Hainan Tropical Ocean University [Grant No. RHDXB201613].

Conflicts of Interest

The authors declare no competing financial interests.

References

[1] Yishao Shi. Theory of enterprise community and its practice in the China. Journal of Tongji University (Social Science Editing), 2001, 12 (4): 41-62.

[2] Tao Meng, Chunhai Jiang. The resource exhausted state-owned enterprises exit barriers and exit pathway analysis. Chinese industrial economy, 2003(10): 5-12.

[3] SASAC. About the reform and development of state-owned enterprises. Xinhuanet.com reported, Beijing, 2012.

[4] Qing Zhang, Zhizhou Xu, Zhongqiu Cai. The resource-based enterprises community vulnerability assessment and control mode. The soft science, 2011, 5: 5-10.

[5] Qing Zhang. Study on mechanism and governance mode of community vulnerability of resource type enterprise. Management world, 2011, 1: 172-173.

[6] Cunfang Li; Linbang Fan; Manzhi Liu. Intervention Factors of Shifting Action of Exhaustible Resource Enterprises Based on Cross-Regional Coupling of Advantage Element and Linkage of Ecological Civilization. Resources Science, 2014, 36(12): 2637-2646.

[7] Cunfang Li, Mei Dong, Qin Wang, et al. The Research Process on Spillover Effect and Intimidation Effect of Interregional Transfer Activities of Resources-Exhausted Enterprises. Economic geography, 2017, 37(3): 106-112.

[8] Hongjie Yang, Changqing Ding. Assessing the Economic Transformation of China's Large-Sized Resources Enterprises: A Case Study of Pingmei Shenma Group. Journal of Nanjing Normal University (Social Science Edition), 2013(5): 46-55.

[9] Shizhang Zheng, Qianhong Wu, Haibo Wang. Ecology: principles, methods and applications. Shanghai: Fudan University press, 1994.

[10] Fuming Zhang. Resource type economy: Research on the internal mechanism and application of interpretation, theory. China Social Science Publishing House, 2007.

[11] Huangjian Kang, Tin Liu, Jun Yang. On the Fragility and managerial Modeof Resource-based Enterprise Clusters from the Perspective of Entrepreneurship. Journal of Jiangnan University (Humanities&Social Sciences), 2013, 12(3): 69-73.

[12] Chongtai Tan. Evaluation was bustling, "Chinese enterprise technical growth mechanism and competitive research". Economic research, 2002, 5: 88-91.

[13] Research on China enterprise technical growth mechanism and competitiveness. Changsha: Hunan people's publishing house, 2002.

[14] Zhenshan Lin, Shuguang Wang. Simulation of the relationship between the collapse of resources shortage and animal enterprises. Acta ecologica Sinica, 2002, 22: 535-540.

[15] Zhenshan Lin. Nonlinear mechanics and atmospheric science. Nanjing: Nanjing University press, 1993.

[16] Zhenshan Lin. Population dynamics. Beijing: Science Press, 2006.

[17] Lihong Yu, Jiachen Li. Resources Listed Enterprises Performance under the Constrains of Duel Externalities. China population resources and environment, 2016, 26(4): 63-72.

 DOI: https://doi.org/10.30564/jgr.v2i4.1871

Author Guidelines

This document provides some guidelines to authors for submission in order to work towards a seamless submission process. While complete adherence to the following guidelines is not enforced, authors should note that following through with the guidelines will be helpful in expediting the copyediting and proofreading processes, and allow for improved readability during the review process.

Ⅰ. Format

- Program: Microsoft Word (preferred)
- Font: Times New Roman
- Size: 12
- Style: Normal
- Paragraph: Justified
- Required Documents

Ⅱ. Cover Letter

All articles should include a cover letter as a separate document.

The cover letter should include:

- Names and affiliation of author(s)

The corresponding author should be identified.

Eg. Department, University, Province/City/State, Postal Code, Country

- A brief description of the novelty and importance of the findings detailed in the paper

Declaration

v Conflict of Interest

Examples of conflicts of interest include (but are not limited to):

- Research grants
- Honoria
- Employment or consultation
- Project sponsors
- Author’s position on advisory boards or board of directors/management relationships
- Multiple affiliation
- Other financial relationships/support
- Informed Consent

This section confirms that written consent was obtained from all participants prior to the study.

- Ethical Approval

Eg. The paper received the ethical approval of XXX Ethics Committee.

- Trial Registration

Eg. Name of Trial Registry: Trial Registration Number

- Contributorship

The role(s) that each author undertook should be reflected in this section. This section affirms that each credited author has had a significant contribution to the article.

1. Main Manuscript
2. Reference List
3. Supplementary Data/Information

Supplementary figures, small tables, text etc.

As supplementary data/information is not copyedited/proofread, kindly ensure that the section is free from errors, and is presented clearly.

Ⅲ. Abstract

A general introduction to the research topic of the paper should be provided, along with a brief summary of its main results and implications. Kindly ensure the abstract is self-contained and remains readable to a wider audience. The abstract should also be kept to a maximum of 200 words.

Authors should also include 5-8 keywords after the abstract, separated by a semi-colon, avoiding the words already used in the title of the article.

Abstract and keywords should be reflected as font size 14.

Ⅳ. Title

The title should not exceed 50 words. Authors are encouraged to keep their titles succinct and relevant.

Titles should be reflected as font size 26, and in bold type.

Ⅳ. Section Headings

Section headings, sub-headings, and sub-subheadings should be differentiated by font size.

Section Headings: Font size 22, bold type

Sub-Headings: Font size 16, bold type

Sub-Subheadings: Font size 14, bold type

Main Manuscript Outline

Ⅴ. Introduction

The introduction should highlight the significance of the research conducted, in particular, in relation to current state of research in the field. A clear research objective should be conveyed within a single sentence.

Ⅵ. Methodology/Methods

In this section, the methods used to obtain the results in the paper should be clearly elucidated. This allows readers to be able to replicate the study in the future. Authors should ensure that any references made to other research or experiments should be clearly cited.

Ⅶ. Results

In this section, the results of experiments conducted should be detailed. The results should not be discussed at length in

this section. Alternatively, Results and Discussion can also be combined to a single section.

Ⅷ. Discussion

In this section, the results of the experiments conducted can be discussed in detail. Authors should discuss the direct and indirect implications of their findings, and also discuss if the results obtain reflect the current state of research in the field. Applications for the research should be discussed in this section. Suggestions for future research can also be discussed in this section.

Ⅸ. Conclusion

This section offers closure for the paper. An effective conclusion will need to sum up the principal findings of the papers, and its implications for further research.

Ⅹ. References

References should be included as a separate page from the main manuscript. For parts of the manuscript that have referenced a particular source, a superscript (ie. [x]) should be included next to the referenced text.

[x] refers to the allocated number of the source under the Reference List (eg. [1], [2], [3])

In the References section, the corresponding source should be referenced as:

[x] Author(s). Article Title [Publication Type]. Journal Name, Vol. No., Issue No.: Page numbers. (DOI number)

Ⅺ. Glossary of Publication Type

J = Journal/Magazine

M = Monograph/Book

C = (Article) Collection

D = Dissertation/Thesis

P = Patent

S = Standards

N = Newspapers

R = Reports

Kindly note that the order of appearance of the referenced source should follow its order of appearance in the main manuscript.

Graphs, Figures, Tables, and Equations

Graphs, figures and tables should be labelled closely below it and aligned to the center. Each data presentation type should be labelled as Graph, Figure, or Table, and its sequence should be in running order, separate from each other.

Equations should be aligned to the left, and numbered with in running order with its number in parenthesis (aligned right).

Ⅻ. Others

Conflicts of interest, acknowledgements, and publication ethics should also be declared in the final version of the manuscript. Instructions have been provided as its counterpart under Cover Letter.

About the Publisher

Bilingual Publishing Co. (BPC) is an international publisher of online, open access and scholarly peer-reviewed journals covering a wide range of academic disciplines including science, technology, medicine, engineering,education and social science. Reflecting the latest research from a broad sweep of subjects, our content is accessible worldwide – both in print and online.

BPC aims to provide an analytics as well as platform for information exchange and discussion that help organizations and professionals in advancing society for the betterment of mankind. BPC hopes to be indexed by well-known databases in order to expand its reach to the science community, and eventually grow to be a reputable publisher recognized by scholars and researchers around the world.

BPC adopts the Open Journal Systems, see on http://ojs.bilpublishing.com

Database Inclusion

Asia & Pacific Science Citation Index

Creative Commons

China National Knowledge Infrastructure

Google Scholar

Crossref

MyScienceWork

BILINGUAL
PUBLISHING CO.
Pioneer of Global Academics Since 1984

Tel:+65 65881289
E-mail:contact@bilpublishing.com
Website:www.bilpublishing.com

ISSN 2630-5070
04
9 772630 507198